Dynamics of a retreating ice sheet: A LiDAR study in Värmland, SW Sweden

Alastair Goodship

Dissertations in Geology at Lund University,
Master's thesis, no 500
(45 hp/ECTS credits)

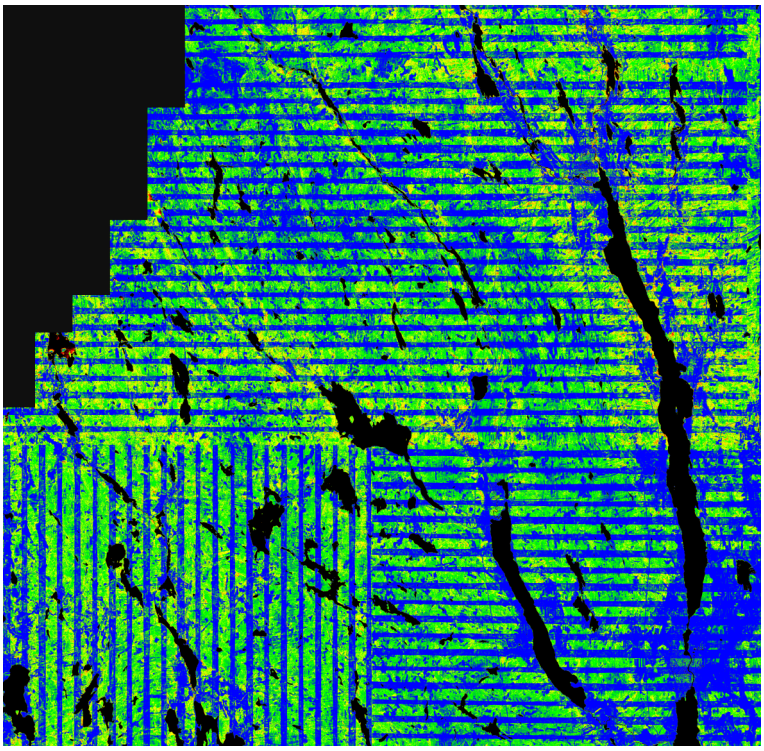

Department of Geology
Lund University
2017

Dynamics of a retreating ice sheet: A LiDAR study in Värmland, SW Sweden

Master's thesis
Alastair Goodship

Department of Geology
Lund University
2017

Contents

Cover Picture: LiDAR density data over study area © Lantmäteriet, i2012/927

ALASTAIR GOODSHIP

Goodship, A., 2017: Dynamics of a retreating ice sheet: A LiDAR study in Värmland, SW Sweden *Dissertations in Geology at Lund University*, No. 500, 33 pp. 45 hp (45 ECTS credits)

Abstract: Värmland in south central Sweden lies across the established zone of aquatic-terrestrial transition of the Scandinavian Ice Sheet margin during its rapid final retreat following the Younger Dryas. Recently acquired LiDAR data across Värmland allows more highly detailed observation and analysis of glacial landforms formed during this stage than has previously been possible. This study synthesises geomorphological mapping of highly detailed digital elevation models (DEM's) and field observations across the region around Torsby in northern Värmland to reconstruct the dynamics of the ice sheet as it retreated. A range of landforms derived from deglacial processes are identified and clearly reflect the change from an aquatic to terrestrially based ice margin. Ice marginal deltas suggest a slowing of retreat at the exact point of aquatic-terrestrial transition. Increased topographic control on ice-sheet flow and pattern of drainage and ice sheet decay is indicated by distribution of streamlined terrain, eskers, outwash material and kettle holes. Hummocky terrain and dead-ice features across low ground and incised valleys suggest persisitance of ice in topogrpahic lows beyond retreat of the main ice front. Combined analysis of identified landforms allows a model for pattern of retreat to be produced that traces the retreating ice sheet margin in far greater detail than has previously been possible in this area.

Keywords: LiDAR, DEM, landforms, glacial, dynamics, ice-sheet

Supervisor(s): Helena Alexanderson

Subject: Quaternary Geology

Alastair Goodship, Department of Geology, Lund University, Sölvegatan 12, SE-223 62 Lund, Sweden. E-mail: alastair.goodship@gmail.com

ALASTAIR GOODSHIP

Goodship, A., 2017: Dynamics of a retreating ice sheet: A LiDAR study in Värmland, SW Sweden *Examensarbeten i geologi vid Lunds universitet*, Nr. 500, 33 sid. 45 hp.

Sammanfattning: Tvärs igenom Värmland i södra-mellersta Sverige sträcker sig den zon där den skandinaviska inlandsisen under sin snabba, slutliga avsmältning efter Yngre Dryas övergick från att mynna i havet till att mynna på land. Nya LiDAR data över Värmland tillåter mycket mer detaljerade observationer och analyser av glaciala landformer bildade i det här skedet än vad som tidigare varit möjligt. Den här undersökningen omfattar geomorfologisk kartering genom detaljerade digitala höjdmodeller (s.k. DEM) och fältobservationer i området kring Torsby i norra Värmland och har som mål att rekonstruera inlandsisens dynamik när den drog sig tillbaka över området. Ett flertal landformer bildade genom glaciala processer har identifierats och de avspeglar tydligt förändringen från en akvatiskt till en terrestriskt baserad isrand. Isranddeltan tyder på en avtagande reträtthastighet precis vid övergången från akvatisk till terrester miljö. Ökad topografisk kontroll av inlandsisens rörelse, dräneringsmönster och avsmältning visas av fördelningen av strömlinjeformad terräng, rullstensåsar, isälvsmaterial och dödishålor. Dödislandskap, t.ex. kames, i topografiska lågområden pekar tillsammans med isälvsrännor på att is låg kvar i låglänta områden efter att huvudisen dragit bort. Genom analys av de identifierade landformerna kan en modell som visar hur isranden har dragit sig tillbaka skapas och det i mycket högre detalj än vad som tidigare varit möjligt.

Nyckelord: LiDAR, DEM, landformer, glacial, dynamik, inlandsis

Handledare: Helena Alexanderson

Ämnesinriktning: Berggrundsgeologi

Alastair Goodship Geologiska institutionen, Lunds Universitet, Sölvegatan 12, 223 62 Lund, Sverige. E-post: alastair.goodship@gmail.com

1 Introduction

1.1 Dynamics

The variations in ice flow rate, ice sheet morphology, hydrology, basal conditions, advance and retreat, and reaction to topography along an ice margin can be referred to as the dynamics of the margin. Historically the study of ice sheet dynamics has been based upon observations of extant ice sheets and glaciated areas and also upon studies of landforms and glacial deposits in previously glaciated regions such as northern Europe and North America. In both cases reliable, consistent observations stretch back ~200 years and have relied on physical investigation and geological mapping of features often complemented by study of aerial photography in later years. In many regions the glacial landforms that are key to determining past ice sheet behaviour are often masked or obscured by forest, later quaternary deposits and by anthropological activities and features.

The study of ice dynamics is of increasing importance given the growing instability and retreat of the Greenland and Antarctic ice sheets in response to global warming. The effort to limit the retreat of these ice sheets is a core pillar of the argument for mitigation of anthropogenic influence on the earth's climate. How these ice-sheets respond to increasing atmospheric and ocean temperatures and varying weather patterns is presently a source of much uncertainty (Vaughan & Arthern 2007).

The dynamics of ice sheets over centennial to millennial scales are reasonably well established but the annual to decadal pattern of ice movement is less well understood. Monitoring of present day ice-sheets shows annual variation and changes more rapid than previously thought possible (Truffer & Fahnestock 2007). There is a need to understand ice sheet margin dynamics on human scales from annual up to centennial. Ice-sheet modelling is the best chance to analyse dynamics on this scale but this relies on input of reliable data both from present day observations across Greenland and Antarctica and from patterns of ice sheet retreat determined from the geological record. The linking of current ice-sheet dynamics and annual to decadal observations to the larger scale pattern of retreat during the termination of the last glaciation is thus a key area of research. Attaining a more detailed model of retreat of extinct ice-sheets will allow better calibration of ice-sheet models focussed on Greenland and Antarctica. As with all geology the past is the key to understanding the present. Recent advances in remote sensing, dating and mapping techniques are providing the basis for more detailed and faster reconstruction of previous ice sheet retreats. The dynamics of these deglaciations can be defined at a much greater resolution than previously possible.

This study aims to demonstrate the ability to use detailed remote sensing data, complemented by field investigation and dating techniques, to reconstruct ice margin movements over a short <200 year timescale. The particular focus is the review of geomorphology and distribution of glacial features in an area in which an ice margin experienced a change from aquatic to terrestrial conditions during retreat.

Advances in remote sensing and observations within the last 20 years has produced a powerful new set of resources for the study of previously glaciated areas. Of particular importance is the advent of Light Detection and Ranging (LiDAR) surveying (Dowling *et al.* 2013). This technique allows detailed profiling of the land surface by, in essence, transmitting a 'pulse' of light towards the earth's surface and measuring the time it takes for the 'echo' to return to the transmitting platform (Rees & Rees 2013). Through use of LiDAR surveying and application of filtering or classification models to the point cloud (Evans *et al.* 2009) high resolution detailed land surface maps known as Digital Elevation Models (DEM) may be produced. These maps are now key resources for the study of glacial features and geomorphology and have seen increasing use in recent years.

Refinement of dating techniques has also enabled a more detailed chronology to be applied to glacial events, notably through the expanded use of luminescence and cosmogenic radioisotope dating (Duller 2004; Balco 2011; Alexanderson & Murray 2012).

1.2 Scandinavian Ice Sheet Deglaciation

The areas that once lay beneath the Scandinavian Ice Sheet (SIS) have been subject to particularly detailed study for the past century and have yielded much of the core knowledge that comprises current understanding of ice sheet dynamics. However, the area that the SIS once covered is vast and much of the terrain is still remote and difficult to access and study. The SIS at its greatest extent was multi-domed and had many major ice-streams flowing through it (Boulton *et al.* 2001). At the last glacial maximum (LGM) the ice-margin covered all of Scandinavia reaching into northern Germany in the south, the North Sea in the west and western Russia in the east (Stroeven *et al.* 2015). Not all areas of the ice-sheet reached their maximum extent at the same time and retreat was equally diachronous (Böse *et al.* 2012). At 20-19 ka the SIS began to retreat as did other ice sheets across the northern hemisphere as the earth warmed (Clark *et al.* 2009). By 12.7 ka the margin had retreated to Lake Vänern in Sweden and ran along the coast of Norway, across the western Kola peninsula in Russia, over the majority of Finland and the Gulf of Bothnia (Stroeven *et al.* 2015). The Younger Dryas interval (12.7-11.6 ka) saw a readvance of the ice margin to the Swedish Middle End Moraine Zone south of Lake Vanern (Fig. 1) (Lundqvist 1995). This advance is also marked by the Salpausselkä moraines in Finland (Saarnisto & Saarinen 2001) and the Ra moraines in Norway along the Oslo fjord (Andersen *et al.* 1995a; Johansson *et al.* 2011). This advance lasted until ~11.7 ka after which the margin began to rapidly retreat. Previous studies (Boulton *et al.* 2001; Saarnisto & Saarinen 2001; Stroeven *et al.* 2015) have indicated retreat rates of 100 m to >250 m per year along the various sections of the margin. The margin around Southern Norway and Western Sweden, where this study is focussed retreated increasingly rapidly following the end of the Younger Dryas, though with periods of standstill recognised by the deposition of end moraines and margin-

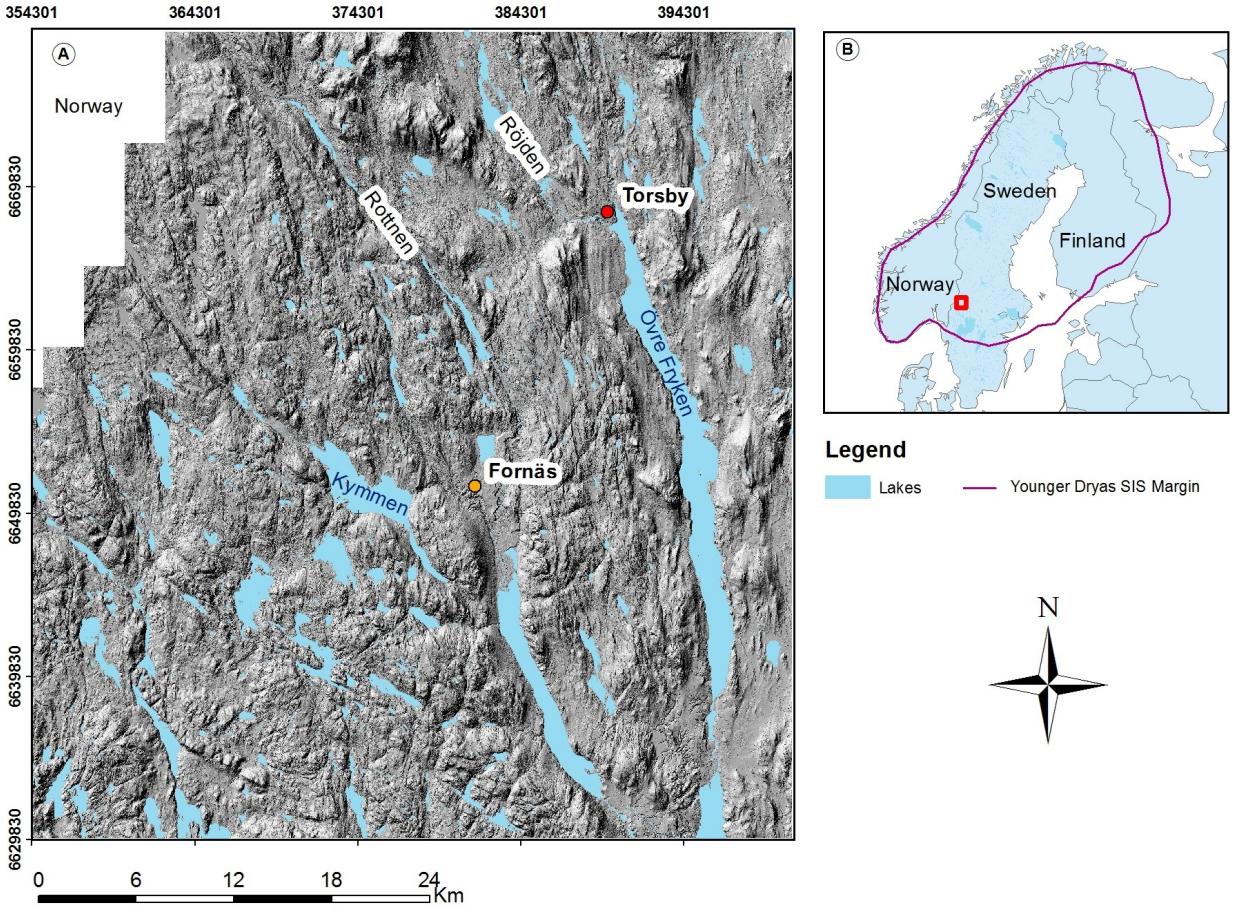

Fig. 1. (A) Overview of study area and location within Sweden along the Norwegian border. Note prominent rivers and NW-SE trend of valleys. (B) Margin of the SIS at the end of the Younger Dryas. Hillshade generated from LiDAR scan data provided by Lantmäteriet, Sweden © Lantmäteriet, i2012/927

al deltas (Solheim 1983; Lundqvist 1995). Outlet of ice via the Norwegian Channel Ice Stream through the Oslo fjord alongside initial aquatic termination of the margin allowed rapid drainage in this area. The rapid loss of ice led to thinning of the sheet and increasing topographical influence on flow patterns. Within just over 2000 years the entire SIS had disappeared altogether. This study is focussed on this period of final retreat, how it is reflected in the geomorphological and geological record and to what resolution the timescale and movement of the ice sheet can be determined in the study area.

1.3 Study Area

The advent of the Swedish National height model (www.lantmateriet.se) has revealed the glacial landscape of the country in detail never seen before. It is now possible to define a greater range and higher concentration of relict glacial landforms. This allows detailed investigation of the dynamics of the retreating SIS.

The study area lies in the county of Värmland in central Sweden around the town of Torsby (Fig. 1). A thorough initial study and mapping of Värmland was carried out by Lundqvist (1958). This area lies in the transitional zone between aquatic and terrestrial ice marginal conditions for the SIS. It is 50 km wide by 50 km long, though tapers to 38.5 km in width in the far north due to a data gap over the border with Norway to the west. Diverse topography surrounds the area with the highlands and mountains of Sweden and Norway to the north and west and the low plains of central Sweden to the south and east. Previous studies in Värmland have established a pattern of retreat to the areas south and east of the study area though these predate the advent of the National Height Model. The work of Lundqvist (1988, 1992, 2003) has traced the retreat from southern Värmland past Lake Vänern and along the Klarälven valley system east of the study area. The region immediately surrounding Torsby has been less well studied. Quaternary mapping has been carried out by the Geological Survey of Sweden (Lundqvist 1958) and recent studies (Zillén *et al.* 2002; Stanton *et al.* 2010) have investigated lakes in the south-east of the study area.

Exposed bedrock is common throughout the study area. Cover till, glaciofluvial, fluvial and aquatic deposits of varying size overlie a bedrock of granites and gneiss with localised occurrences of dolerite, rhyolite and dacites. A large fault zone runs through the west of Värmland and the study area, trending NW-SE to NNE-SSW. Most major valleys follow this trend. Two large rivers the Rottnen and the Röjden flow from

NW to SE across the area (Fig. 1). The Rottnen flows through an incised valley in the NW before flowing south to into Mellan Fryken lake. The Röjden flows southwards before flowing into Övre Fryken to the south of Torsby.

2. Methods

2.1 LiDAR Data Analysis

LiDAR scans covering the study area were obtained from the Swedish national mapping agency Lantmäteriet (www.lantmateriet.se). These scans form part of the National Height Model (Nationell Höjdmodell) for Sweden, which has an average vertical accuracy of 0.1 m and pixel resolution of 2 m allowing detailed study of the landscape. Scans are pre-processed to present a "true'' ground level without urban areas, wood cover and anomalous recordings.

ArcGIS10.3™ was used to generate two main sets of hillshade models; one with an illumination azimuth at 135° and the other 225°, running parallel and normal to the general lineament trend as described in the methods of Smith and Clark (2005) . Both models had an illumination angle of 40° and vertical exaggeration of 5. Individual hillshades of varying illumination were generated where required to better define features identified from the 135° and 225° models. The DEM's were also reclassified and overlaid on to hillshade layers within ArcMap™ to plot the marine limit for 190 m within the study area. The SWEREF99_TM projection was used for all mapping analysis within ArcGIS.

Hillshade models were used for both initial landscape analysis of the area and subsequent review following field investigations. Geomorphological features were identified and marked using points, polylines or polygons. Mapping and interpretations were carried out by one person thus limiting user bias.

2.2 Feature Classification

These geomorphological features were assigned to five principal groups being 1. Moraines, 2. Streamlined Terrain, 3. Eskers, 4. Dead Ice and glacial melt features and 5. Dunes and post glacial features. The five categories were chosen due to their unique landform features and associations, formation processes and specific use in determining past ice margin position, ice flow direction, ice-bed processes and deglaciation pattern. Detailed categorisation is set out below.

2.2.1. Moraines

Moraines provide a definite position of the ice margin and are often prominent features in the landscape. Due to the nature of glacial erosion the moraines present in a previously glaciated area generally represent maximum extent and pattern of retreat from the last glaciation. These features are thus key for glaciological investigation (Bennett 2001) and reconstructing the positon of the ice-margin during retreat. There are several types of moraine with each representing a distinct formational process. Benn and Evans (2004) provide a thorough description of the varying types. This study particularly focusses on end moraine types that appear as prominent ridges and features within the landscape and are readily identifiable within hillshade models.

De Geer moraines have been studied in detail via the National Height Model by Bouvier *et al.* (2015); (SGU 2016) and occur throughout the south of the study area. Mapping of southern Värmland by Lundqvist (1992) identified several moraines in areas neighbouring the study area. These features were treated as established ice-marginal 'anchor points' in this study from which the more detailed focus of this investigation could be launched. In the case of De Geer moraines these were mapped as part of the hillshade analysis and then compared to the study by Bouvier *et al.* (2015). Moraines or moraine like features identified by this LiDAR study were included in this group.

2.2.2. Streamlined Terrain

Streamlined features are a distinct set of subglacial landforms used for determining ice sheet and ice bed dynamics (McClenaghan 2001; Benn & Evans 2004). They are representative of both erosional and depositional processes at the ice-bed interface and indicate ice-flow direction (Dowling *et al* 2016). Landforms occur in areas ranging from 10's to 1000's of metres in length and breath. LiDAR data is particularly adept at showing these areas (Möller & Dowling 2015) and allows for identification of intermediate to large scale individual features. Streamlined features were identified according to the classifications of Benn and Evans (2004) and Sugden and John (1976).

2.2.3. Eskers

Eskers are key identifiers of previous ice sheet presence and orientation during retreat. They often occur alongside distinct marginal and deglaciation features including hummocks, drainage channels and deltas. Eskers were identified according to widely accepted characteristics of sinuous or broken ridges standing above or distinct within surrounding terrain. Recent similar LiDAR based studies (Peterson & Smith 2013; Johnson *et al.* 2015) were referred to for comparison of identified eskers and to aid initial classification of esker type prior to field investigations.

2.2.4. Dead-ice and glacial melt features

Three sub-categories were used for this group of features. All are key for tracing a retreating and decaying ice margin.

2.2.4.1 Hummocky Terrain

Hummocky terrain represents areas of sediment deposited from stagnating ice. Varying patterns of terrain exist and styles of deposition are best summarised by Benn and Evans (2004). The depositional process most commonly associated with hummocky terrain formation is of the irregular deposition of supraglacial material during the down-wasting of stagnant ice.

Areas of hummocky terrain were identified by typical morphology of conical, linear and irregular shaped mounds readily identifiable within the hillshade models. Hummocks are largely composed of diamict material though this cannot be revealed via

LiDAR data. These characteristics were taken into account during field investigations. Reference was made to the study of Möller and Dowling (2015) that presented an area of hummocky terrain in Sweden studied via the same LiDAR dataset and thus provided at least a basic analogue for initial landform analysis and classification.

2.2.4.2 Outwash Plains and Pitted Outwash

During deglaciation large volumes of meltwater flow from the ice margin. Within this meltwater is transported large volumes of sediment of predominantly sand and gravel size that can be classed as 'outwash material'. The entrained sediment is deposited in front of the retreating ice margin either in valleys and basins or across wide plains. Material can also be deposited across delta topsets in shallow water. Wide, flat areas of outwash material deposition are referred to as outwash plains. Often this outwash material is deposited around blocks of dead ice that have been left behind by the decaying ice sheet. These ice blocks can become entirely buried by sediment. As the dead ice blocks melt they remove the support for overlying sediment which then falls or flows into the depressions or 'pit' left by the melting ice. This results in the formation of pitted outwash with holes of varying scale distributed across an outwash plain.

Outwash plains were identified in the hillshade models via their 'smooth' surface texture relative to neighbouring bedrock and position within natural drainage points such as valleys and plains. Pitted outwash was identified by the presence of pits or kettle holes within the outwash plain surface.

2.2.4.3 Drainage Channels

Channels are indicative of meltwater outflow from beneath and around ice margins and as such are common features within a deglaciated landscape. They may take the form of incisions into bedrock, shallow surficial channels or erosional features within underlying tills and sediments.

Determining origin and relative age of drainage channels is difficult due to post-glacial processes. For this reason only channels that could be confidently linked to glacial processes due to positioning in landscape and/or relationship to other glacial features were highlighted.

2.2.5 Dunes and post glacial features

This group includes features such as dunes and raised beaches that though not directly related to active glacial processes have a link to subsequent processes that occur following deglaciation. Dunes often form within glacial deposits shortly after deglaciation e.g. at Brattforsheden proximal to the study area (Alexanderson & Fabel 2015) and are thus evidence of landscape evolution and adaption immediately following ice retreat.

Features were identified according to established morphologies and with reference to the summary of glacial features identified from the National Height Model data set by Peterson and Smith (2013), in particular dune and highest coastline HCL appearance within hillshade models.

General analysis of HCL position within the study area was also carried out via DEM reclassification in ArcGIS. A baseline HCL of 190m was modelled according to the established HCL elevation in the region (Zillén *et al.* 2003). Further analysis and modelling was carried out upon completion of fieldwork. Elevation data was compared directly with the DEM's to check accuracy and agreement between the two data sets.

2.3 Quaternary Mapping Analysis

Quaternary deposit maps up to a scale of 1:25000 were obtained from the Geological Survey of Sweden (SGU 2016) for the study area. Specific maps for the study area were generated from the SGU website (http://www.sgu.se/produkter/kartor/kartgeneratorn/). Following initial evaluation of field sites, ArcGIS layers of the quaternary deposit data were obtained from the SGU Jordarter database (https://maps.slu.se/). These maps predate the National Height Model and as such have varying levels of detail. Maps from the area are based on air photo interpretation and field observations along the road network. As such there are large areas with limited or no previous field observations. Nonetheless the Jordarter database provides a valuable overview of quaternary deposit distribution and aids in identification of key glacial and geomorphological features.

Following initial geomorphological analysis of the LiDAR data using DEM's, quaternary map layers were overlaid and compared to the features that had been identified. Correlating glacial features were marked and clear quaternary deposit boundaries added to the LiDAR based map. Features that were present only on the quaternary deposit map were compared alongside the relevant DEM and added to the working layer where correlating evidence could be identified.

2.4 Field Mapping

Field work was carried out by the author in September 2016. Features identified through LiDAR and quaternary map data were ranked in order of priority for mapping and investigation. Accessibility was also taken into account to allow for most efficient use of time. The key field observations and data to be recorded for each feature and area were morphology of targeted feature and surrounding terrain, sedimentary composition of feature with detailed descriptions where possible/applicable, sedimentary structural features, bedrock prominence and structure, vegetation cover and type where applicable. Field positions and elevation were recorded using a Garmin Map62S handheld GPS unit with accuracy of ±3 m. Sedimentary logs were constructed from delta and esker sections when accessible. Some sites were found to be inaccessible due to poor or no road access. Overview photos were taken of all sites visited and detailed photos taken where necessary.

2.5 Optically Stimulated Luminescence (OSL) analyses

Two samples were taken for OSL dating from bands in

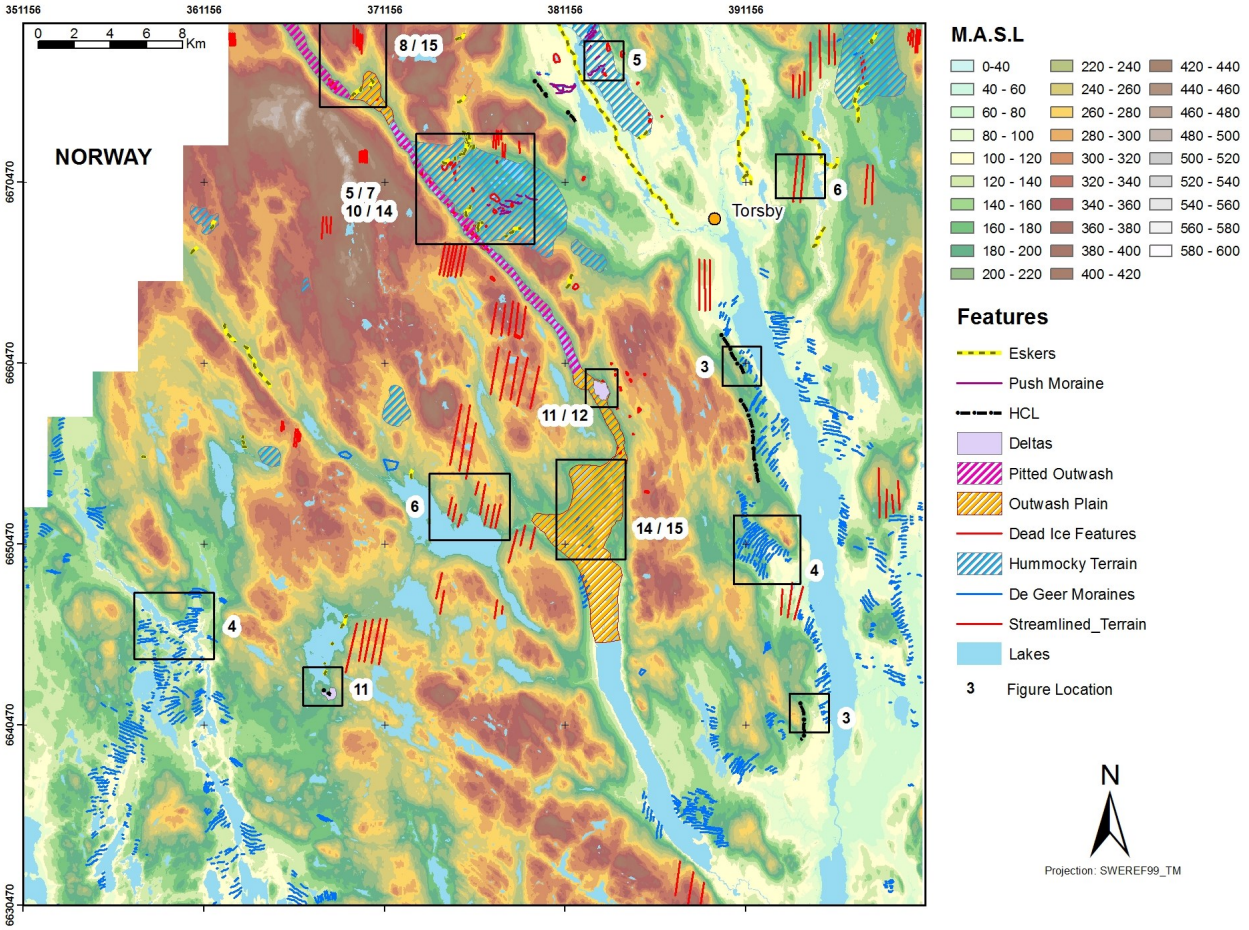

Fig. 2. Overview of study area and field site investigation. Black outlines indicate areas shown in detail by following result figures. Hillshade generated from LiDAR scan data provided by Lantmäteriet, Sweden © Lantmäteriet, i2012/927.

a sand rich esker feature (Fig. 7). Samples were collected using a plastic tube wrapped in opaque plastic tape. These were then wrapped in plastic sheet and opaque tape and remained sealed until opened under darkroom conditions. The aim of sampling was to determine whether the feature formed under aerial or sub-glacial conditions As such a full OSL dating analysis was not required and instead the rangefinder dating method of Roberts *et al.* (2009) was used. Samples were a mix of quartz, feldspar and other minerals. Analysis was carried out at Lund University. In line with the Roberts *et al.* (2009) protocol only untreated material was analysed. Three 8 mm aliquots per sample were measured with a shortened Single Aliquot Regeneration (SAR) protocol (Murray & Wintle 2000, 2003) with post-IR-blue stimulation (Banerjee *et al.* 2001), three regenerative doses but recuperation and no recycling.

3. Results

Combined LiDAR data analysis and field investigations within the study area reveals a number of glacial features with a clear variation in distribution around the highest coast line (HCL) and within regional structural features. Twenty-one field sites have been investigated and revealed important sedimentological, structural and geomorphological characteristics key to reconstructing the pattern of deglaciation in the study area An overview of identified features is given in Fig. 2 and particular zones of interest that are discussed later in this section are outlined with associated figures shown.

3.1 Highest Coastline

The highest coastline for the study area is generally accepted to lie at ~190 m.a.s.l (Zillén *et al.* 2003). Fig 3 shows the marine limit for this elevation. The south of the study area lies close to or below the HCL apart from a central area of high ground. The central and north-western zone is predominantly above. In the north the low ground between the Rottnen and Kläralvern rivers lies below the highest coastline. Distinct beach ridges are visible in the hillshade models along the eastern extent of the study area (Fig. 3b, 3c). These ridges are difficult to observe in the field.

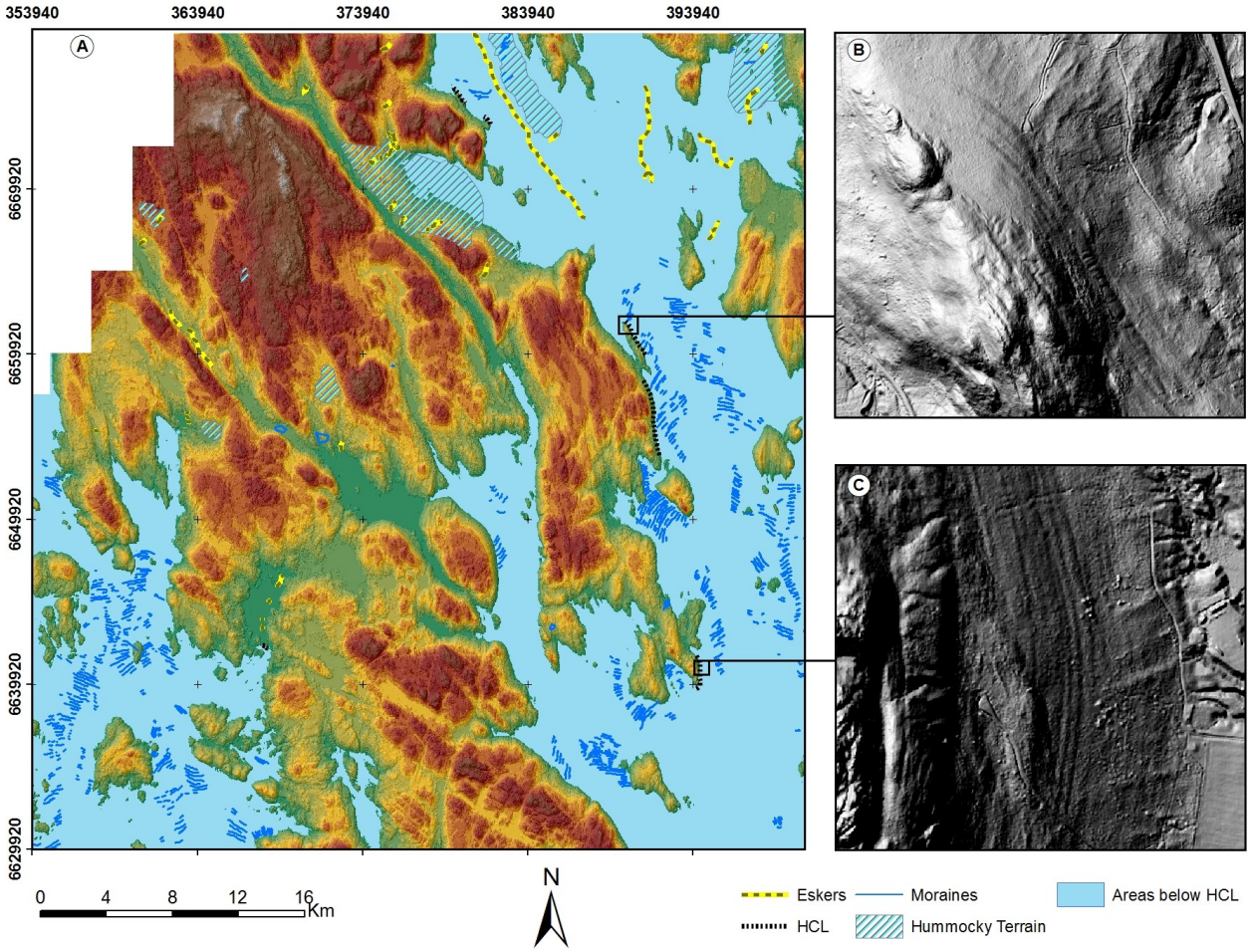

Fig .3. (A) Study area with extent of 190 m highest coastline. De Geer moraines all fall below the highest coastline. (B & C) Former shorelines are visible as distinct ridges within hillshade models. Hillshade generated from LiDAR scan data provided by Lantmäteriet, Sweden © Lantmäteriet, i2012/927.

3.2 Moraines

3.2.1 De Geer Moraines

De Geer moraines are distributed across the southern half of the study area. These all lie below the HCL (Fig. 3) and clearly follow the formerly aquatic areas. They are clearly identifiable within the hillshade models (Fig. 4) as was also determined by Bouvier et al. (2015). The moraines are predominantly concentrated along narrow valleys in the south of the study area. Moraine ridges are on average 10-15 m wide and range from 20 m in length to over 3 km. Ridges show a NE-SW trend along western valley sides and NW-SE along eastern valley sides. Spacing between ridges is roughly 120-250 m and the path of retreat can be determined over several kilometres (Fig. 4). The orientation of the ridges indicate formation of pronounced calving bays in a generally ENE-WSW trending ice margin. Moraine ridges become increasingly concentrated in valleys towards the north with lateral extensions into neighbouring high ground absent. The succession of De-Geer moraines ceases ~4 km south of Torsby. It is noticeable that the wide area below the HCL in the north east is lacking in De Geer moraines compared to other areas below the HCL. Moraines may have formed in this area but have been subsequently buried beneath marine silt and sand or did not form at all. De Geer moraines are much more difficult to positively identify in the field though. Investigations of a number of sites including that shown in Fig. 4B reveals a slightly undulating terrain with isolated 30 cm-60 cm boulders on small mounds. Despite this the clear definition of features shown within the hillshade models and their wide distribution in previously subaquatic marginal areas allows a high level of confidence in their positive identification as De Geer type moraines.

3.2.2 Push Moraines

A series of small push type end moraines are present below the HCL in the north of the study area (Fig. 5B, 5C). These small 14-35 m wide ridges run parallel to sub-parallel to presumed ice margin for up to 500 m. No field investigation of these features was able to be carried out so a definitive identification is unable to be given. The orientation of the ridges does though sug-

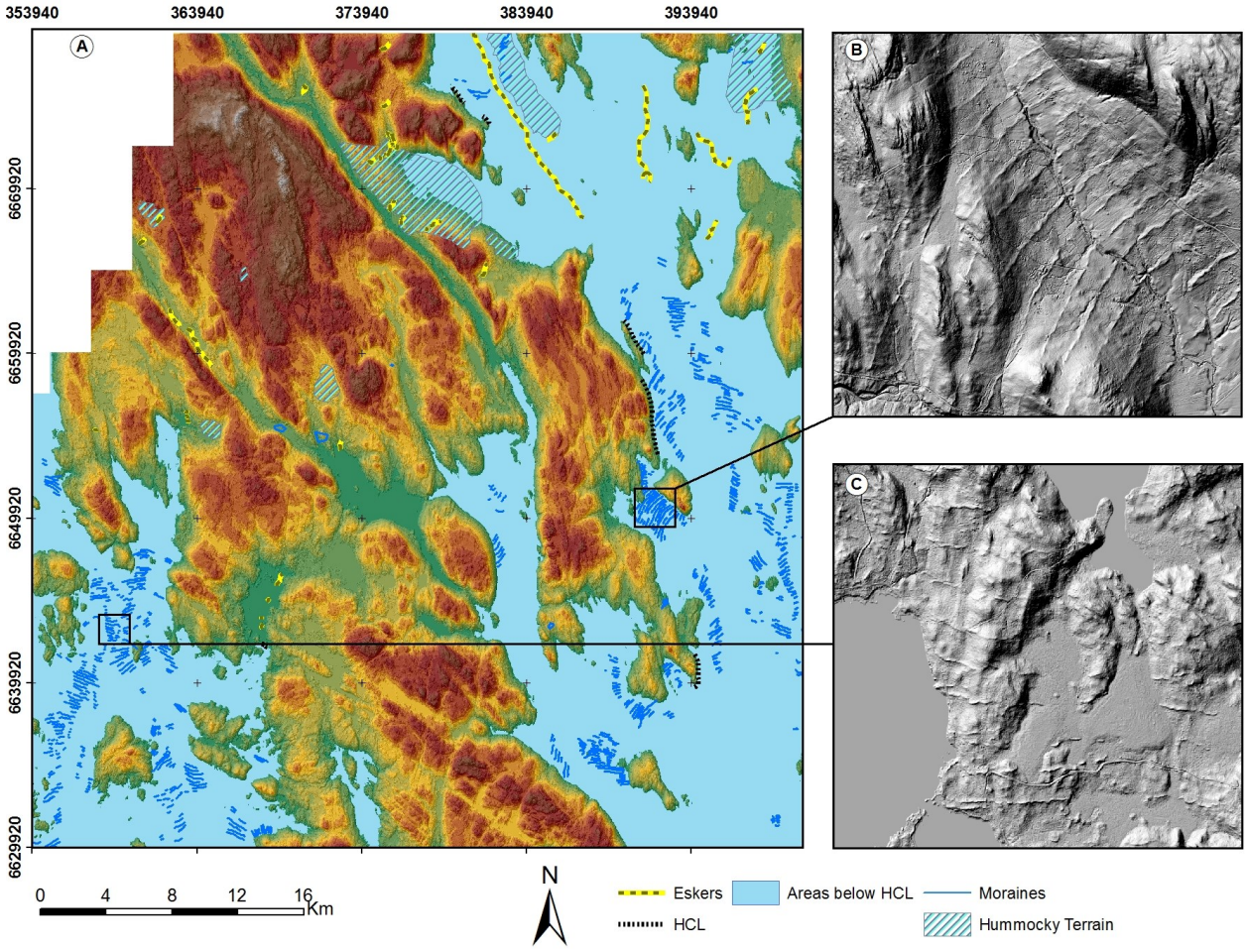

Fig. 4. (A) Wide distribution of De Geer moraines across southern half of study area. (B) Note increased concentration in valleys towards the north. (B & C) Moraine orientation with sets of NE-SW and NW-SE trending ridges indicates the presence of calving bays within the ice front. Hillshade generated from LiDAR scan data provided by Lantmäteriet, Sweden © Lantmäteriet, i2012/927.

gest formation either at the edge of an ice lobe or valley glacier or within crevasses on a stagnating margin.

No other major terminal or lateral moraines were identified in the study area other than the De Geer moraine sequence below the HCL.

3.3 Streamlined Terrain

Streamlined features are present across the study area. Features take the form of rock-cored drumlins, fluting and scoured terrain amongst general streamlining within cover till. Features fall in similar classes to those observed by Möller & Dowling (2015) but aerial distribution in the landscape differs. Smoother surface texture in streamlined areas suggests a greater sediment and till thickness than neighbouring areas. The long axis of features trends NNE-SSW in the south but moves to a straight N-S orientation towards the north of the study area (Fig. 6). A majority of identified features exist well above the HCL and often on elevated ground of 250+ m.a.s.l. This suggests better preservation in elevated areas indicating a lack of dead ice remaining during deglaciation and no ongoing sedimentation that could distort or cover these features. The active ice margin likely retreated steadily over these areas and they were then isolated from later deglacial processes that obscured streamlined forms at lower elevations. Possibly cold-based ice covered some areas of higher ground during late glaciation as the ice sheet thinned and pressure at the base of the ice sheet decreased also acting to preserve streamlined bedforms.

3.4 Eskers

North of Torsby are found a number of prominent long flat-crested ridges many kilometres in length along the bottoms of NW-SE trending valleys (Fig. 2, Fig. 4). These features are surrounded in large areas by outwash material. The valleys in which they lie trace the profile of the major NW-SE trending structural lineations in the region. The features are interpreted as tunnel-fill eskers deposited in sub aquatically terminating R-channels as described by Brennand (2000).

Smaller 100 m—200 m long features are found across flat areas generally above the HCL with orientation ranging between N-S and WSW-ENE. These features are both flat-crested and sharp-crested with

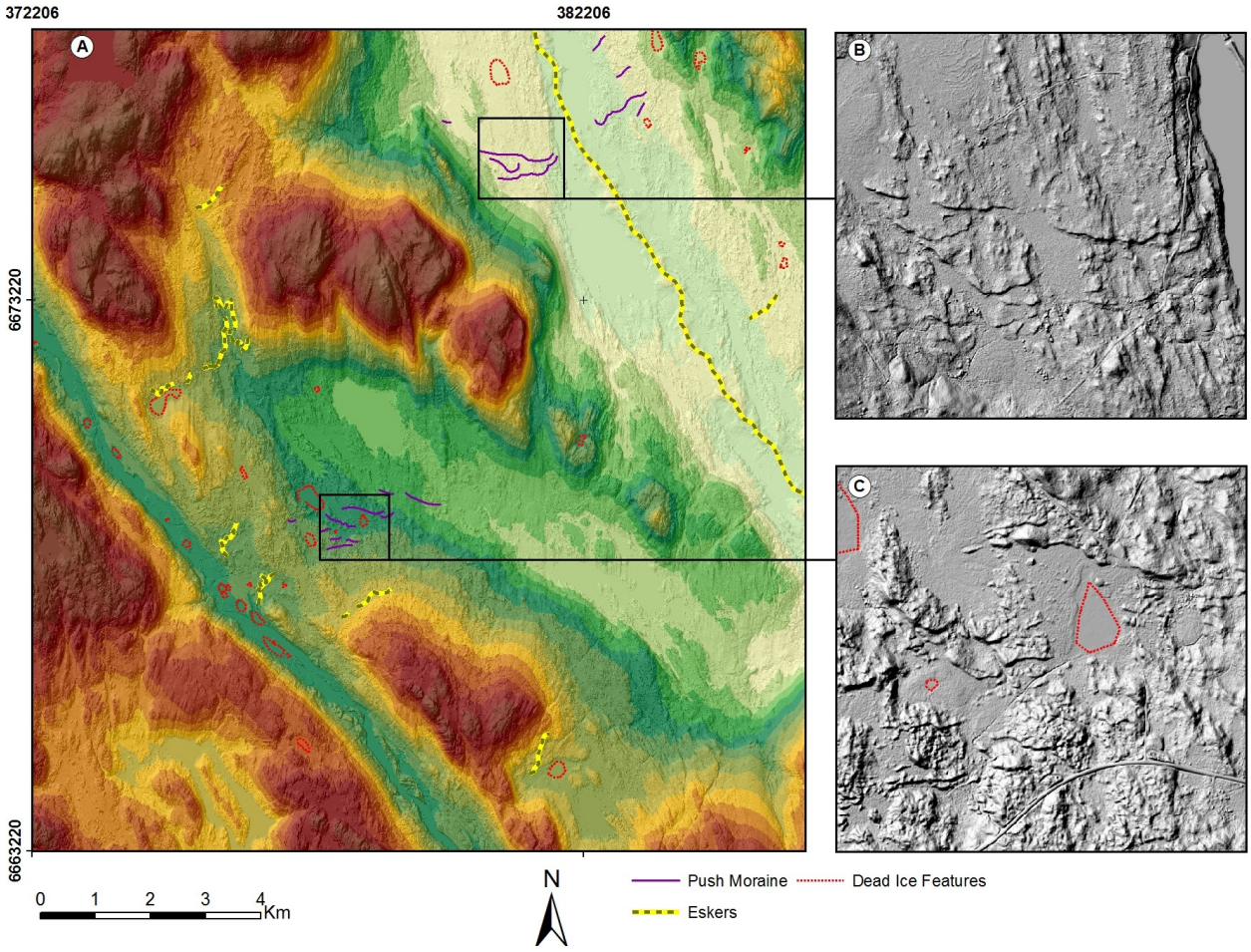

Fig. 5 . Push moraine ridges in low ground in north of study area. Ridges in (B) formed below 50 m to 100 m water depth. Ridges in (C) formed below 10 m to 30 m water depth and at the HCL. Hillshade generated from LiDAR scan data provided by Lantmäteriet, Sweden © Lantmäteriet, i2012/927.

variation between boulder and gravel rich composition. The smaller features likely also represent tunnel-fill eskers in areas of lateral drainage towards the main valley or local bedrock depressions. Presence of cobbles and boulders within the main esker body indicates high energy environment of deposition. Boulders of 50 cm to 150 cm in size lying on the surface represent material deposited during down-wasting of overlying ice in areas above the HCL and dropout from drifting icebergs below the HCL. A general WSW-ENE boundary between De Geer moraine and esker rich areas can be observed in Fig. 2 and Fig. 4. This indicates a change of drainage pattern and basal hydrology with shallowing water depth and transition to terrestrial conditions and also better surface preservation following deglaciation above the HCL.

Three sinuous, sharp crested features that run perpendicular to major eskers are present to the east of the Rottnen River in low ground. These features lie oblique to parallel to the assumed ENE-WSW trending ice margin. They are unique within the study area and stand proud from surrounding hummocky terrain and range from ~650 m to 1.8 km in length. Field investigations revealed a distinct composition set out below. Section locations are shown in Fig. 7.

A fourth sharp crested ridge is present further north along the valley (Fig. 8). This ridge also tracks NE-SW but lacks the sinuous profile of the three further south and is located up against the valley side next to an area of outcropping bedrock. Field investigation found this feature to be 40 m above the valley floor and deposited within a stepped bedrock terrain. A 70cm hole excavated on the top of the feature revealed a fine, well sorted brown sand overlying a gravelly sand layer A thorough investigation of internal composition and morphology could not be done due to time constraints. The eastern side of the feature is very steep and drops away sharply into the valley below. It is likely the stepped structure of underlying bedrock anchors the material in hollows between bedrock steps. Material that does not sit above the bedrock falls away into the valley. This feature is likely an esker that formed along the valley side with meltwater channelled along the bedrock surface onto which material was deposited.

3.4.1 Section S01

This section is from one of the sharp crested features in the northern part of the study area (Fig. 7B.). The

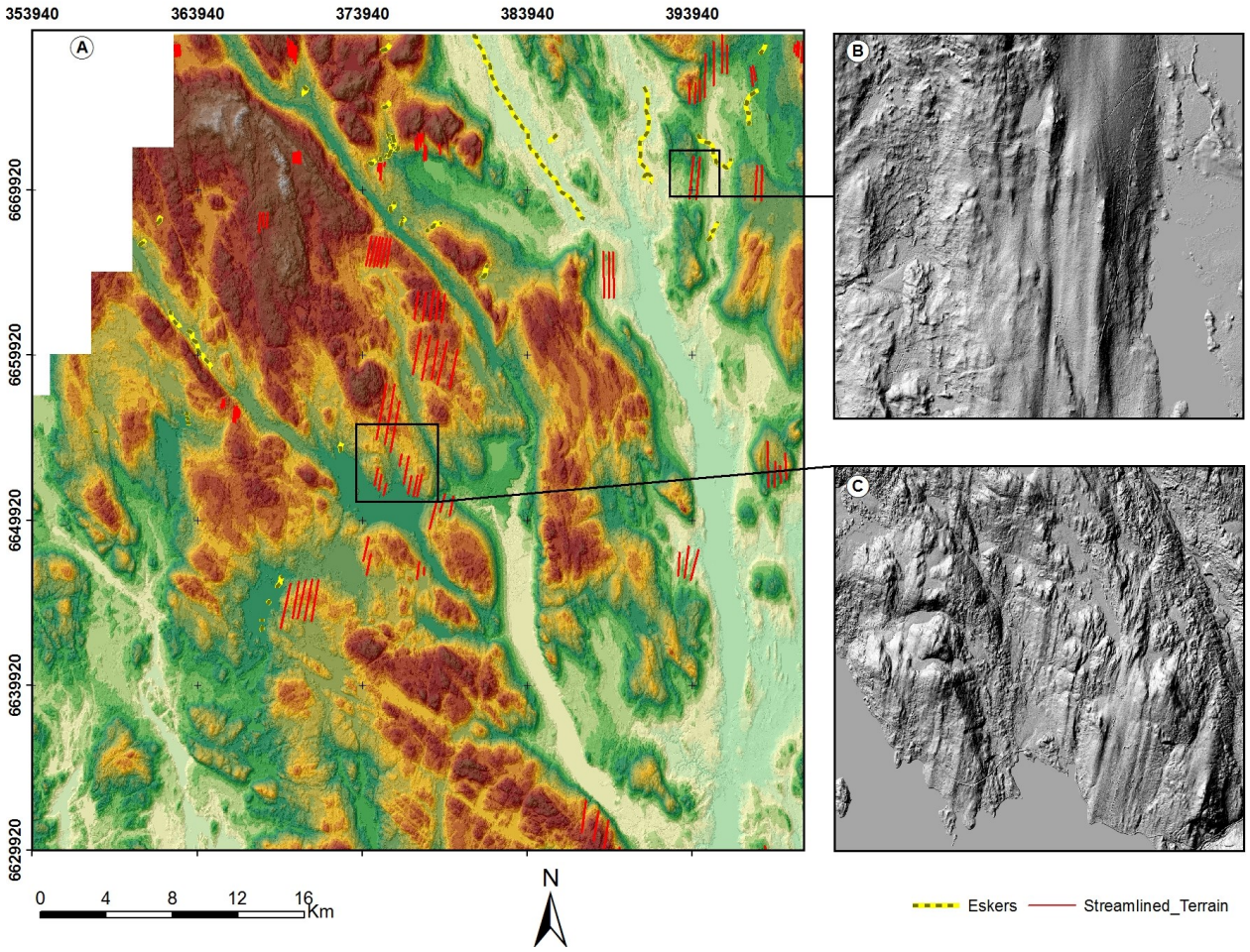

Fig. 6. (A) Streamlined terrain within study area. Prominent features including rock cored drumlins present over elevated ground but not visible in lower areas. Note shift from NNE-SSW to N-S orientation towards north of study area between (C) and (B). Hillshade generated from LiDAR scan data provided by Lantmäteriet, Sweden © Lantmäteriet, i2012/927.

corresponding log is shown in Fig. 9.

3.4.1.1 Section Description

Bed 1: This grey-brown sandy diamict forms the base of the excavated section. The bed has a fine sand matrix with sub-angular to rounded gravel clasts of 1-5 cm evenly distributed throughout.

Bed 2: Clast supported sandy gravel. The basal contact is gradational to sharp. Sub-angular, 8-10 mm clasts of crystalline rock comprise >85% of material with a coarse quartz sand matrix between. The bed is red-orange in colour.

Bed 3: Fine-medium grained well-sorted red sand. The basal contact is gradational.

3.4.1.2 Interpretation

The beds lack any internal structure and show varying amounts of sorting. The situation on the side of an esker suggests deposition at the same time or as a final stage of melting of surrounding ice. The material likely is derived from gravity flows and fluvial processes during the late stage melting of supporting ice. These flows acted to drape the esker in less sorted material. The sediments in the beds 1 and 2 were deposited in an environment in which finer material could be winnowed out likely through steady flow of meltwater, though not at high energy. The sand in bed 3 at the top of the section may be deposited in a final waning flow along the esker channel or may be a later cover of sand deposited during final deglaciation and ice melting.

3.4.2 Sections S02 and S03

Sections S02 and S03 are from another of the sharp crested features in the northern part of the study area (Fig. 7C). These sections represent two sides of the same feature so interpretations are combined. The corresponding logs are shown in Fig. 10.

3.4.2.1 S02 Section Description

Bed 1: Massive fine to medium grained sand. 1 cm thick horizons of dark silt rich material are found at 60 cm and 69 cm height and show gradational contacts with surrounding massive sand. Isolated, 1-4 mm rounded crystalline rock fragments are present throughout the bed.

Bed 2: Massive, normally graded orange-yellow coloured gravelly sand. Sharp basal contact with Bed 1. Flat, angular 1-3 cm clasts of friable rock are supported in a medium to fine grained sandy matrix.

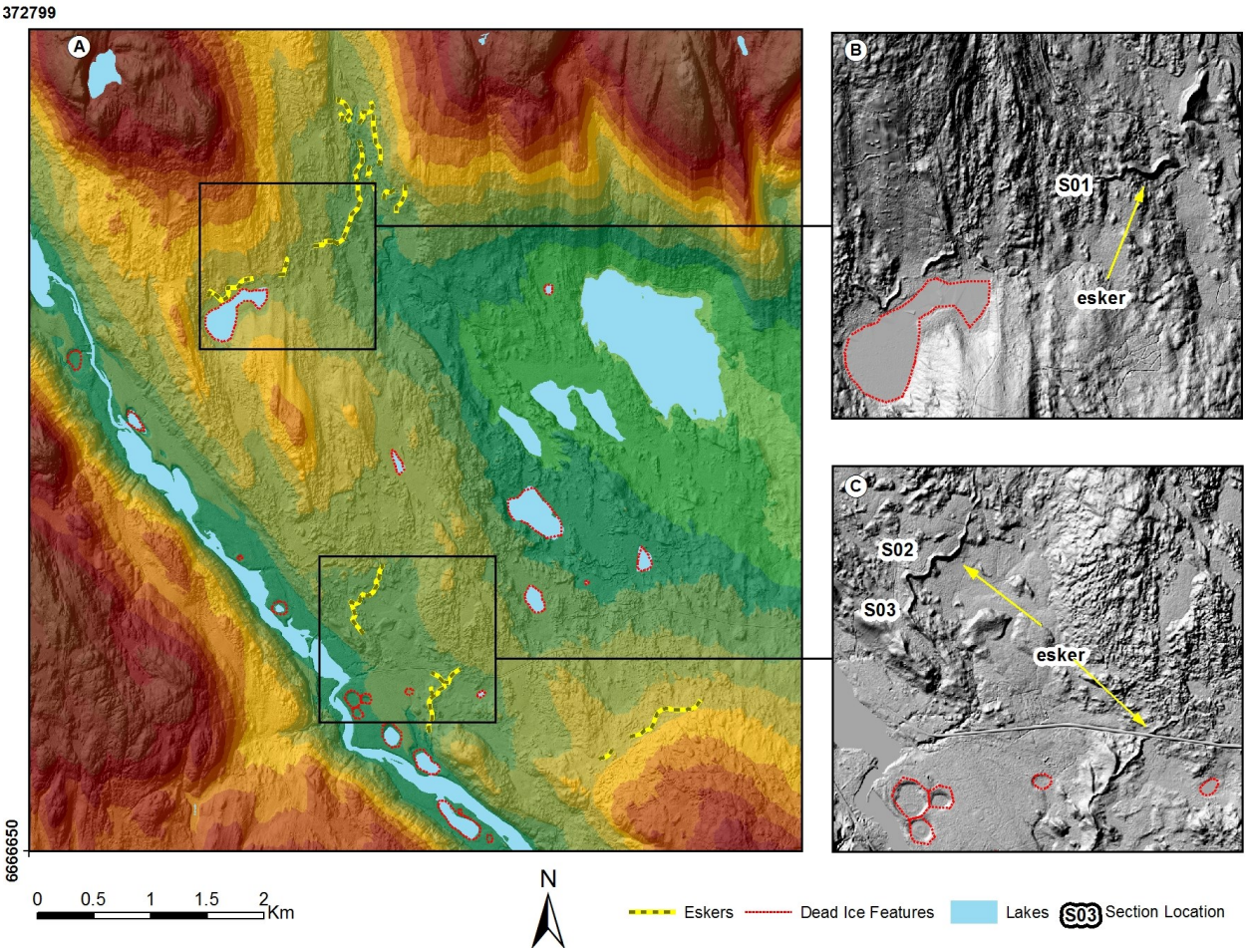

Fig. 7. (A) Prominent esker features. Ridges run NE-SW sub-parallel to assumed ENE-WSW ice margin. (B & C) Distinct sinuous sharp crested profile of eskers is clear with surrounding hummocky terrain and outwash material. Hillshade generated from LiDAR scan data provided by Lantmäteriet, Sweden © Lantmäteriet, i2012/927.

Bed 3: Massive, rounded, crystalline, 1-4 cm gravel clasts are evenly distributed throughout a medium to coarse sand. The crystalline material is very red, possibly garnetiferous. Rare, 1-3 cm very rounded mafic clasts are present. Base of bed shows sharp contact. Orange-yellow sands dominate at the lower half of the bed with grey sands comprising >50% of material towards the top.

3.4.2.2 S03 Section Description

Bed coset 1: Light brown, fine to medium grained sands. Isolated 2-6 mm dark brown bands. Layer shows planar cross lamination but structure is less well defined in comparison to overlying beds. Trough cross bedding present in centre of bed indicating a flow towards the west.

Bed coset 2: Medium to fine brown sands. Gradational basal contact with bed 1. Cross bedding prevalent throughout bed. Orientation of beds indicates a ENE-to-WSW flow direction. Bedding sets have dark brown top bands with 1-2 mm rounded clasts on the bed toes. Beds are stacked one on another in a series of wedges and are increasingly steep towards the base of the bed. Deformation structures are present along the upper contact with 5-10 cm wide faulted blocks present.

Bed coset 3: Medium to coarse sand. Sharp faulted basal contact with bed 2. Fault blocks are 5-10 cm wide. The bed shows wedge shaped cross bedding throughout, dipping towards the NE.

Bed 4: 0.5 cm-3 cm sub rounded crystalline clasts with medium to coarse grained infilling sand. Inversely graded. Bed has sharp basal boundary with bed 3. Gravel clasts are dominantly comprised of garnet-gneiss.

Bed 5: red-orange fine to medium grained sand. Bed is massive and shows irregular basal boundary with bed 4.

Bed 6: Grey medium grained sand. Bed is massive and shows sharp basal boundary with bed 5. Organic and re-worked material overlies this bed.

3.4.2.3 OSL Analyses

Two samples OS01 and OS02 were taken from section S03 for OSL analysis. These are indicated in Fig. 10B. OS01 was taken from cross-bedded, well sorted medium to fine sand in the centre of the section. OS02 was

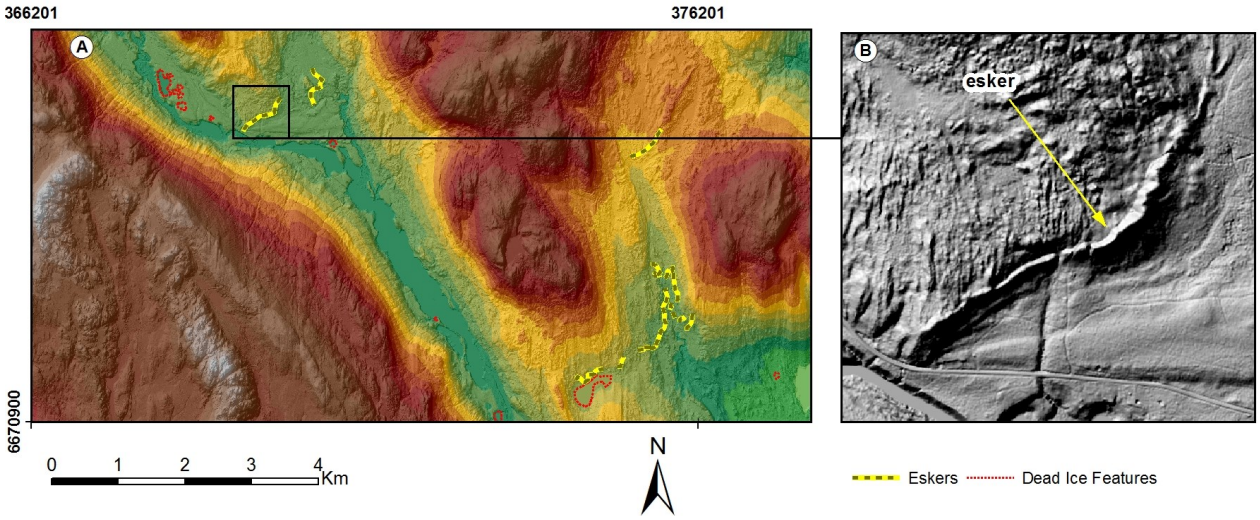

Fig. 8. (A) Sharp crested transverse esker on western side valley with small outwash plain below. (B) Esker sits upon 'stepped' bedrock outcrop likely aiding its stability and preservation. Hillshade generated from LiDAR scan data provided by Lantmäteriet, Sweden © Lantmäteriet, i2012/927.

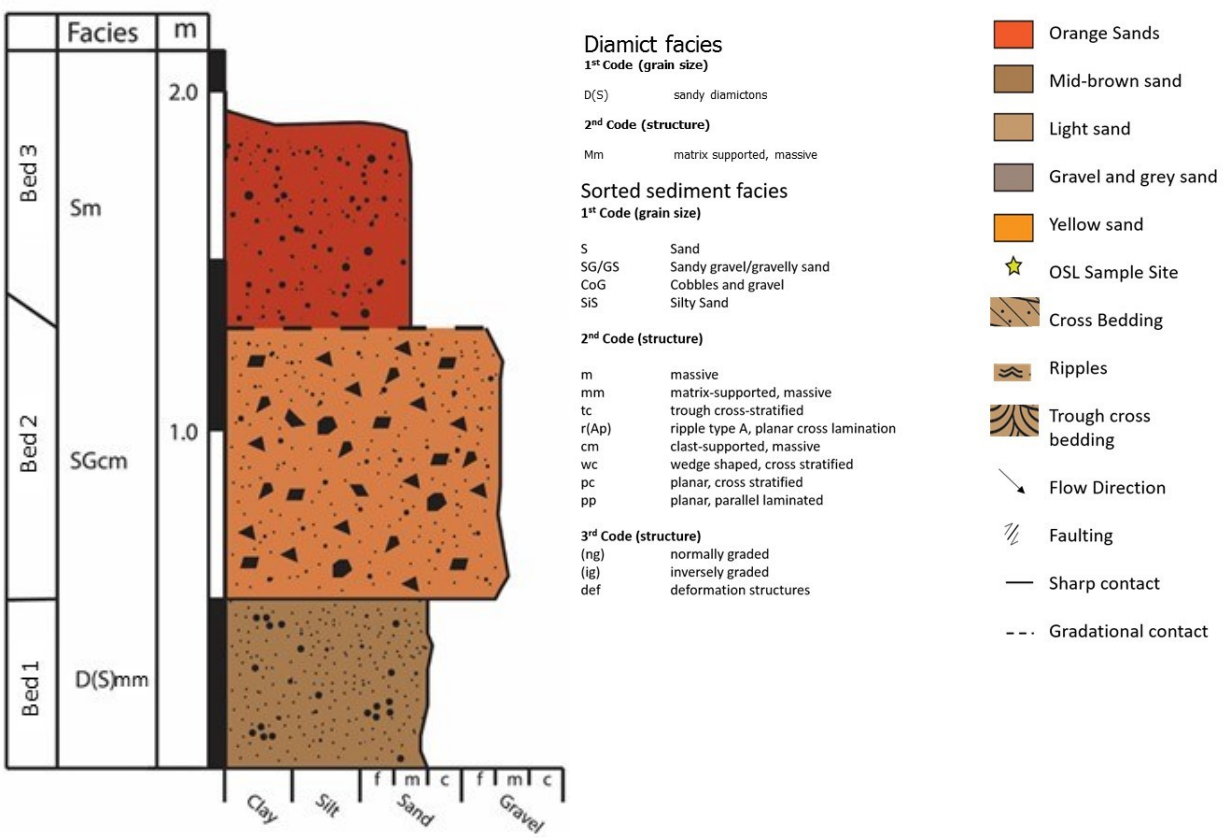

Fig. 9. Section through drape of melt out material overlying esker in Fig. 6B at site S01.

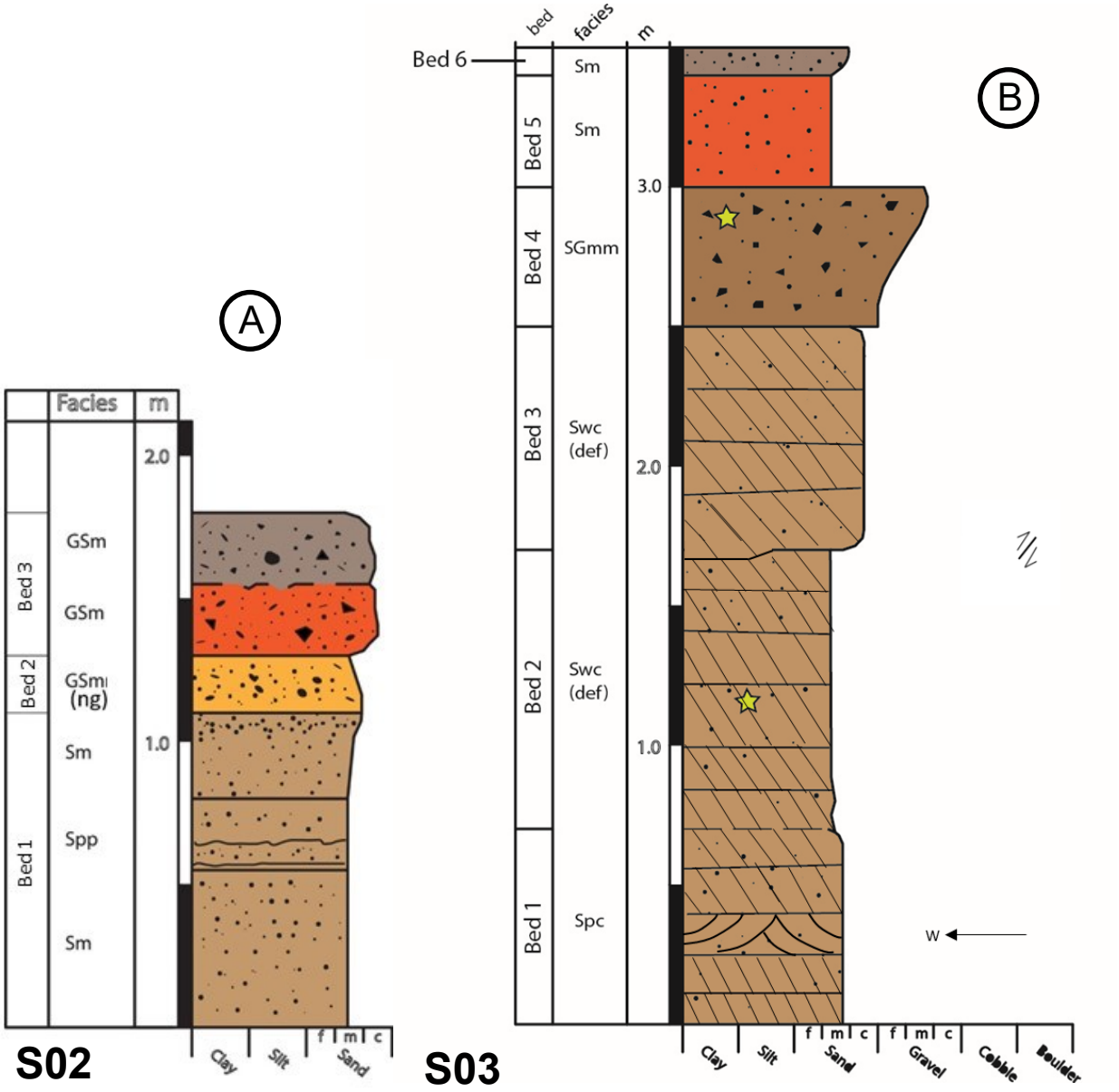

Fig. 10. (A) S02 Section through northern side of esker in Fig. 6C (B) S03 Section through western side of esker in Fig. 6C. Yellow stars indicate position of OSL samples taken to aid determination of supra or subglacial deposition.

taken from a sandy gravel layer near the top of the section. Equivalent dose values returned were 272 ± 45 Gy for OS01 and 269±26 Gy for OS02. These results can be compared to those of Alexanderson & Fabel (2015) at Brattforsheden. In their case equivalent values were obtained from poorly bleached glaciofluvial deposits. This indicates that the features analysed here must have been deposited sub-glacially or in a sub-aquatic setting where a level of shielding prevented 'zeroing' of electron traps in the test material.

3.4.2.4 Interpretation Section S02 and S03

Stacking of beds is evidence of an enclosed depositional area such as a crevasse or tunnel. The presence of normal and trough cross bedding illustrates that flow direction in the tunnel varied.

The sediments were deposited in a sub-glacial conduit, likely an R-channel or deep crevasse from a generally low energy water current. The sequence is not of a typical esker indicating unique conditions prevailing at the time of formation. Gravels at the top of the section represent an increase in energy and possible final infill of the tunnel. It is suggested the sequence represents one of two depositional settings/systems. 1. a seasonal meltwater derived deposit with initial low energy conditions giving way to high energy as the melt season continues, represented by fine sand giving way to gravel. 2. a multi seasonal feature representing a period of standstill and steady decay within the ice, supplying a constant stream of meltwater before decay begins to speed up and higher energy conditions prevail. Small fault blocks illustrate a degree of syn-sedimentary slumping and instability but the feature shows good internal strength with no

large scale deformation. It is fair to assume that ice support was present for a significant period postdepositionally to prevent severe slumping. Within the context of this study these three features are classed as 'transverse-eskers' owing to their morphology and assumed position parallel to an ice front.

3.5 Deltas

Two ice-marginal deltas were identified within the hillshade models (Fig. 11A). The two deltas, one in the south-west and the other in the north of the Rottnen Valley, have a width of ~450 m and ~630 m respectively. The delta in Fig. 11B was visited during fieldwork. It lies ~10 km SW of Torsby around Lake Gäddtjärn (Fig. 11 and 12). An exposure that could be cleaned and logged was found in a disused quarry. The GPS derived elevation of the present quarry floor places it at 189 m.a.s.l (±3 m). The delta sequence rising from the quarry floor is ~10m in height.

3.5.1 S04 Section

The upper part of the delta in Fig. 11B was cleaned and logged for c. 2 m (Fig. 13).

3.5.1.1 Section Description

All the beds in the section except bed 9 dip to the west.

Bed 1: Massive bed of cobbles with a gravel matrix. Gravel clasts 0.3-3 cm, cobbles 6-15 cm. Both cobbles and gravel are well rounded. Crystalline material dominates.

Bed 2: Massive sandy gravel. Gravel is sub-rounded with clasts of 0.3-3 cm. Sand is coarse-granular. Bed shows sharp basal contact with bed 1.

Bed 3: Cross bedded fine to medium grained sands. Gradational bedding in cross bedded bands with finer sand present on toes of beds and at upper bed boundary. Bed shows sharp basal contact with bed 2.

Bed coset 4: Medium to fine grained sequence of normally graded 4-10 cm thick beds. The bed has a sharp basal contact with bed 3.

Bed coset 5: Cross-bedded medium and fine sands. Alternating of 10-15 cm wide medium grained beds with 5-10 cm thick normally graded medium to fine grained beds. The bed shows a sharp basal contact

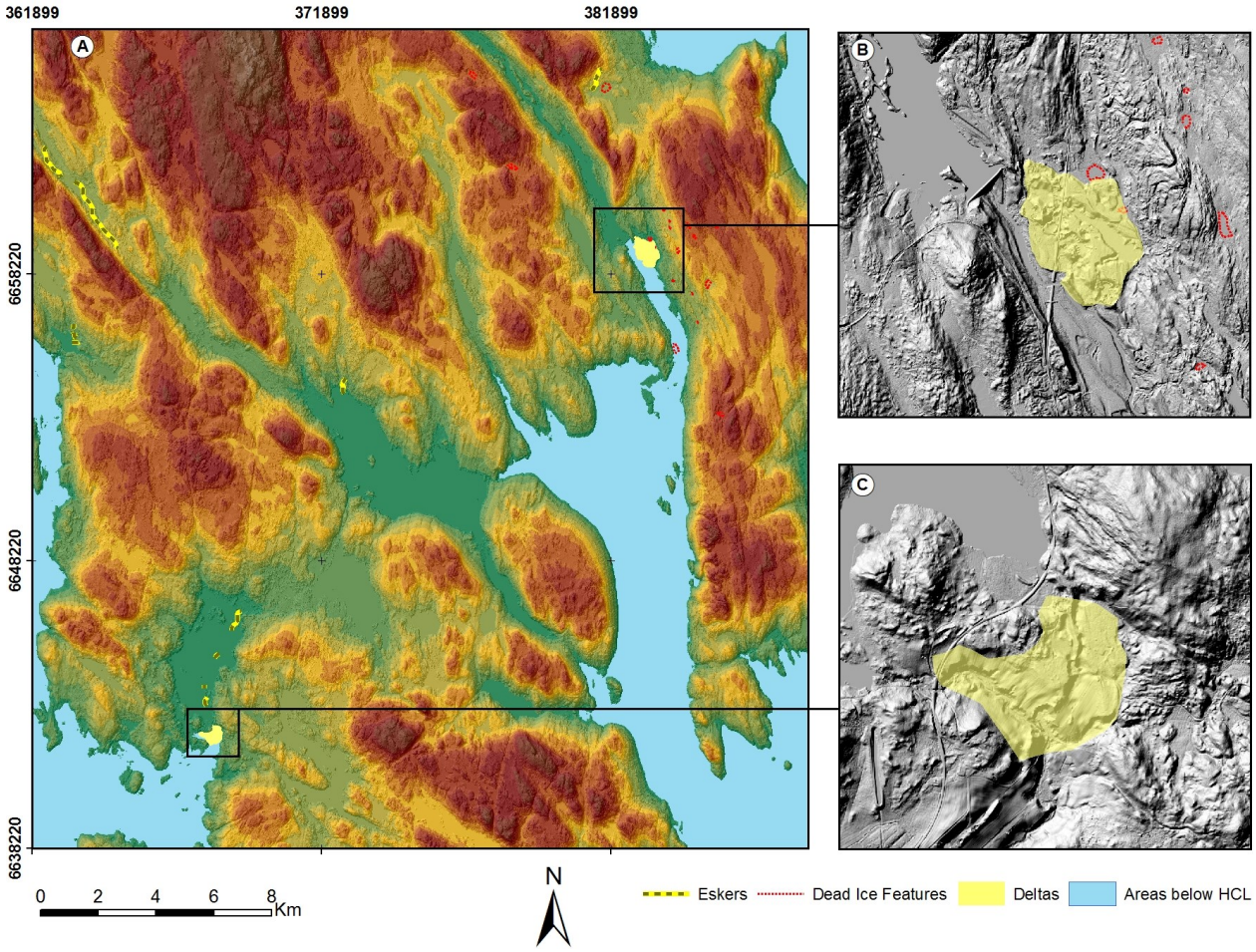

Fig. 11. (A) Overview of delta locations within the study area. (B) Delta outline on eastern side of Rottnen river valley at HCL (C) Delta location at HCL in the SW of study area. The two deltas are of similar size and represent a period of slowed ice margin retreat at the point of aquatic-terrestrial transition. Hillshade generated from LiDAR scan data provided by Lantmäteriet, Sweden © Lantmäteriet, i2012/927.

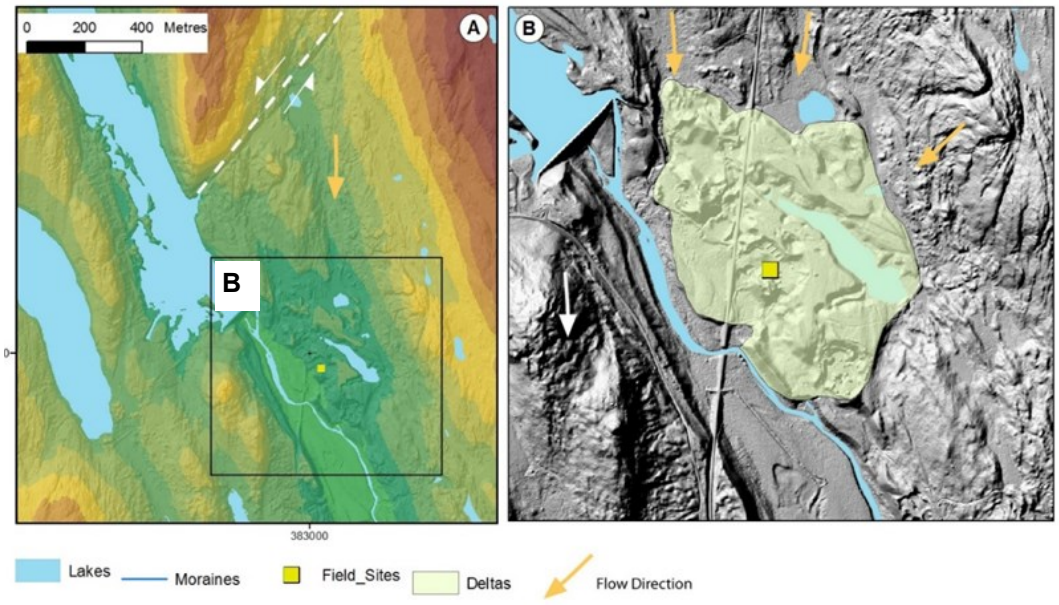

Fig .12. Enlargement of the delta shown in Fig 11B. (A) A faulted bedrock block to the north of the delta on the eastern bank of the Rottnen Valley. The fault is shown as a white dashed line and clearly shows an offset between two ridges. (B) Drainage channels indicating flow of water and transported sediment from the N and NE into area around the delta. Hillshade generated from LiDAR scan data provided by Lantmäteriet, Sweden © Lantmäteriet, i2012/927.

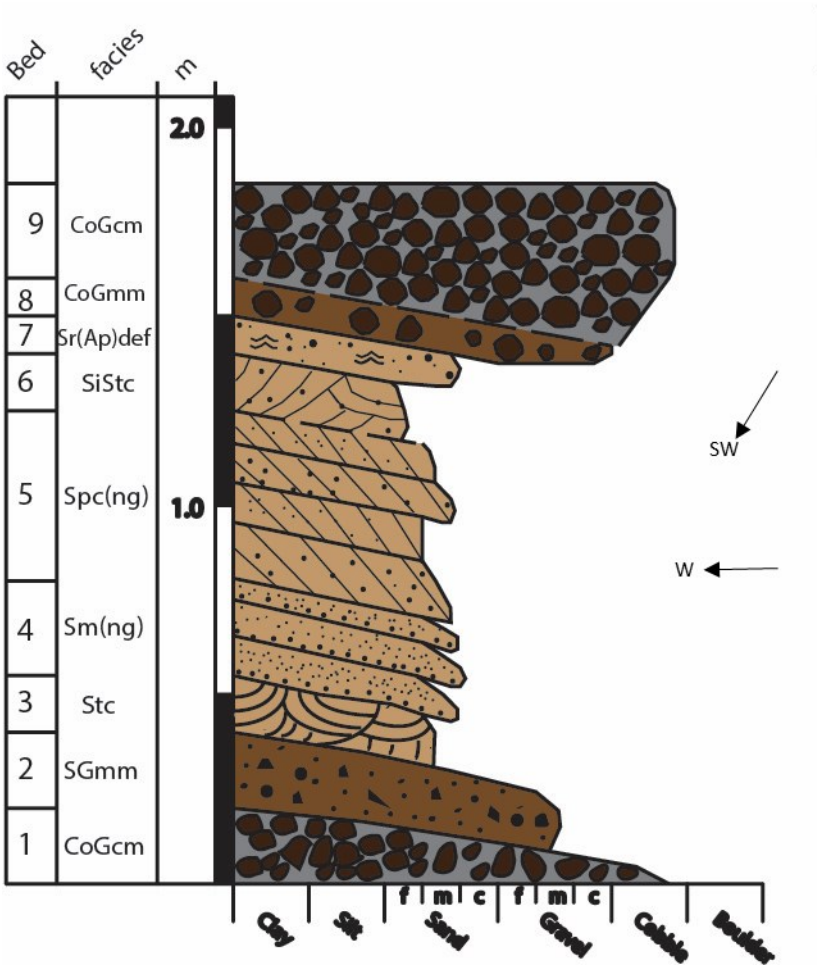

Fig. 13. Section through uppermost 2 m delta shown in Fig. 10B at the HCL. At least 8 m of material underlies this section but could not be exposed and logged. All beds but upper cobble rich layer are dipping west following the slope of the valley side.

with bed coset 4.

Bed 6: Cross bedded fine sands with dark brown silt along toes of beds. Sharp basal contact with bed 5.

Bed 7: Cross bedded and rippled medium sand. Cross beds present at base and transform to ripples towards upper boundary. Beds at base of bed dip to the west at ~20° before shallowing of angle towards the top of the bed as ripples appear.

Bed 8: Massive matrix supported cobble gravel. Fine sandy matrix . Cobbles are sub rounded and 10-20 cm in diameter .The bed has a gradational contact with underlying bed 7.

Bed 9: Massive clast supported cobble gravel with a medium sand matrix. Gravel clasts are rounded and 0.5-2 cm. Cobbles 10-20 cm and rounded. Bed is flat lying.

3.5.1.2 Interpretation

The section is very short and possible interpretation and conclusions that can be drawn are thus limited. There is though evidence to suggest the environment in which individual beds were deposited.

Cobble beds are often more commonly associated with bar aggradation in a stream or river. However, the prominent dip on all but bed 9 suggests more likely deposition along a delta slope. The roundness of the cobbles in both bed 1 and bed 9 suggests the material was entrained over a long period or may be redeposited material possibly from a basal till. The presence of the cobble rich bed 1 at the base of the sequence suggests an initially high energy environment. Flat lying bed 9 has a much larger size of material and the gradational basal contact with bed 8 suggesting an environment of increasing energy across the period of deposition.

Bed 9 is interpreted as part of a topset succession formed in shallow water across previously deposited foresets. Cobble rich layers are common for bars forming between channels and could be argued to indicate deposition in a subaerial environment. There is evidence of channels on the surface of the deposit but much has been disturbed by quarrying activities.

Gravels in a granular matrix, bed 2, that overly bed 1 show weakening flow conditions possibly supporting a slumping of previously deposited coarser material and formation of a gravity flows.

The gravity flow feature in bed 7 may represent cyclical foreset slumping of the type described by Benn & Evans (2004) and be indicative of initiation of turbidity flows down the delta front. The succession of fining upward beds and evidence of gravity flows is a common deltaic feature. The limited height of the exposure precludes making a definitive interpretation, however, the most likely setting for deposition of beds 3 to 7 is at an ice marginal delta.

The section appears to show the very upper foresets and the topsets of an ice marginal Gilbert type delta that formed at the edge of still active ice typical of that described by Lønne (1995). The delta was deposited on a steep valley side so there would have been a sharp depth gradient towards the valley centre. The section is very short and beds are thin (12 cm-45 cm) and thus may represent deposition over a short period. The prominent westerly dip of the beds lends to the identification as part of a delta. The top of the exposure was recorded at 199 m.a.s.l (±3 m) and this places it at or just above the HCL in the area.

3.6 Dead Ice and Glacial Melt Features

Prominent dead ice features are found within valleys and across lower elevations in the study area.

3.6.1 Outwash Plain

A large 1.5 km wide sedimentary deposit plain is present in the Rottnen river valley (Fig. 14C) 3.8 km south along the valley from the delta in section 3.7 (Fig. 11B). The valley widens at this point into what was once a large bay just below the HCL. The plain is marked by a series of terraces built high above the current river channel (Fig. 14C). The hillshade model reveals a series of braided paleo-streams on the surface (Fig. 14C). The size of this feature, its distinctive terraces and relict braided channels suggests a previous period of rapid deposition into the basin. Outwash material was channelled rapidly down the river valley until it entered deeper water and was deposited. This resulted in the building of a delta within the bay. An outwash plain eventually formed on the top of this delta and is the feature visible in the hillshade model. This bay eventually became isolated during isostatic rebound and formed a lake. Input of material reduced and the river incised into the outwash plain and delta beneath.

3.6.2 Pitted Outwash

This topography is present within the Rottnen River valley within the study area. Kettle holes with widths of 30 m - 300 m+ are present in the area around the sand rich eskers shown in Fig. 7. Pitted outwash topography is evident by the gently sloping plateau surfaces in the valley interspersed with holes where dead ice has since melted to leave a depression or small lakes (Benn & Evans 2004). Varying levels of terraces are present within the valley with kettle holes concentrated in upper terraces. The upper terraces represent the immediate post-glacial surface across which dead-ice was prevalent. Post glacial erosion into this surface and underlying outwash material has produced the sequence of terraces now observable and left the pitted surface isolated above the present river level. The kettle holes present as clear depressions in the landscape, often forming isolated small ponds and lakes.

3.6.3 Hummocky Terrain

Hummocky areas are present in the northern section of the study area generally at wider, low elevations or flatter areas bounded by highland. Significant areas are shown in Fig. 2 and Fig. 14A. Conical mounds 10-50 m in diameter are interspersed with elongate ridges 30-150 m in length and stand 5-20 m proud of surrounding terrain. Distribution of mounds and ridges is irregular. Large zones of hummocky terrain are present in

wide areas both above and below the HCL in the north east of the study area indicating the presence of grounded ice that later decayed over a longer period and deposited supraglacial material. Water depth in these areas was from 100 m to 60 m so a large area of ice would have had to remain grounded after active margin retreat to prevent significant deposition of lacustrine sediments.

3.6.4 Drainage Channels

A number of drainage channels are identified across the study area. Discerning an origin during deglaciation or within later quaternary events directly from the hillshade model is not always possible and field checks on identified sites were limited due to other glacial features deemed more significant and worthy of investigation. The generally shallow till cover and concentration of sedimentary deposits within lower areas amongst bedrock outcrops also makes channels difficult to define Identified channels range in size from 30 m to 200 m+ in length and 10 to 30 m in width. The pattern of drainage suggested by the hillshade models is of flows from high elevations into valleys, where ice may have still been extant, lowland plains and lower lakes and depressions. In the case of drainage into valleys and lowland plains the water and suspended material flowed into areas of both active and dead ice both sub-glacially and supra-glacially. This is evident by the presence of eskers, kame and kettle terrain and hummocks.

3.7 Dunes

Two small dune sets were identified (Fig. 15). Both lie on top of sand rich outwash plains along the Rottnen river valley. The situation on the top of the plains suggests late stage formation once the ice margin had retreated further north. Bedding features shown in Fig 16 present a classic cross bedded dune form. The features identified in Fig. 15C may reflect the profile of underlying glacial features that anchored dune formation and have since been buried as they do not present a classic dune profile. Assuming that the dunes are transverse, they reflect a prevailing NW wind direction.

4. Discussion

The combination of LiDAR derived DEM and hillshade model analysis alongside field investigation of

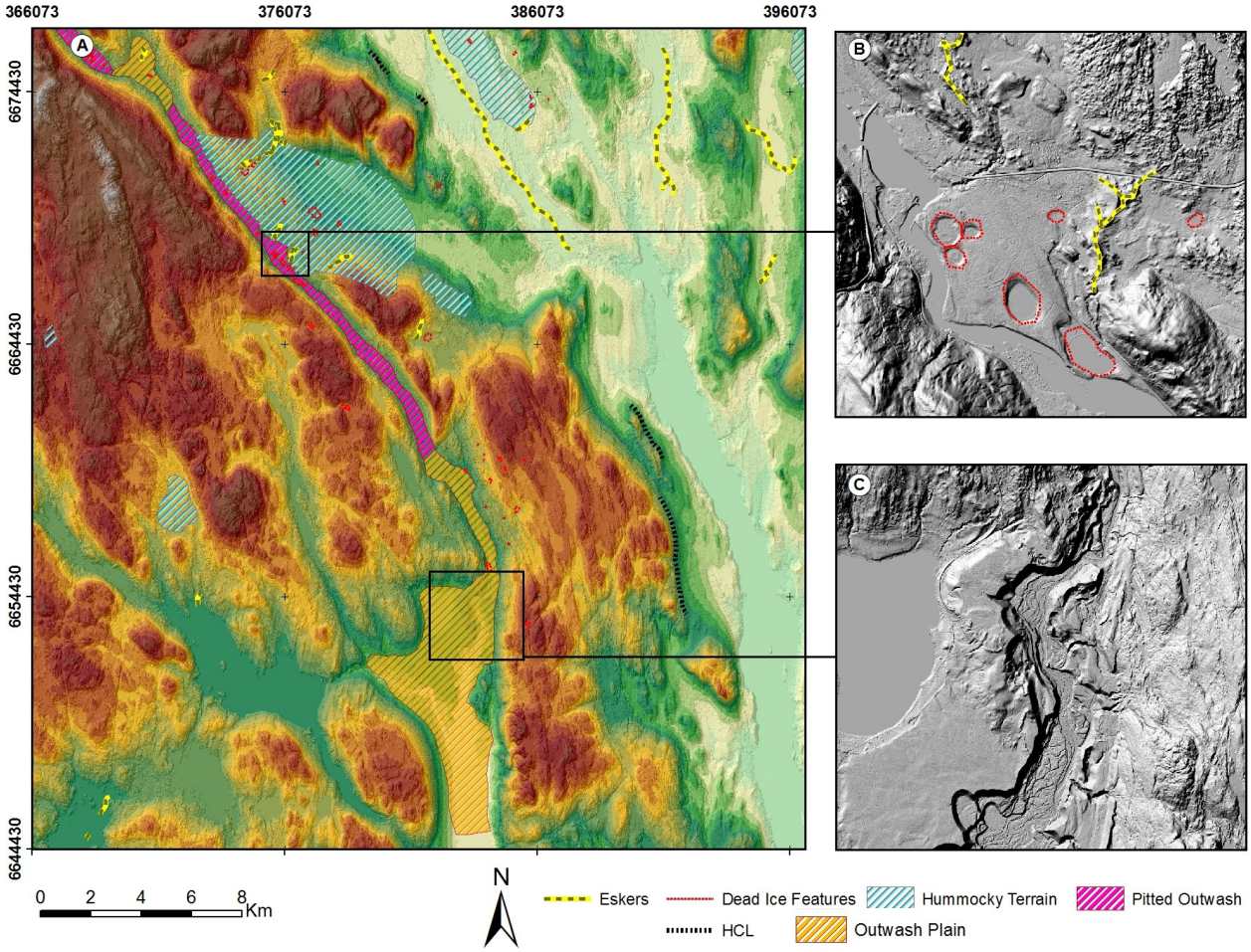

Fig. 14. (A) Hummocky terrain and pitted outwash within and around Rottnen river valley. (B) Note largest area of hummocky terrain on lowland to east of valley. (C) Large lake likely formed from kettle hole is present in NW of outwash plain. Hillshade generated from LiDAR scan data provided by Lantmäteriet, Sweden © Lantmäteriet, i2012/927.

the study area has revealed a clear range of both terrestrial and aquatic glacial landforms. Features deposited within active and stagnant ice have been identified and linked to processes both sub-glacial and supra-glacial.

The study area clearly lies across the zone across which the SIS margin retreated from the Yoldia Sea and became largely terrestrially based. This transition is reflected in the changing type of glacial landforms and deposits along a generally N-S line of glacial retreat.

The first part of this discussion focuses on the formation of the landforms identified within this study and what this indicates about the position and dynamics of the ice sheet margin in the study area. The features are discussed beginning with those below the HCL through those at the aquatic-terrestrial margin and finally those above the HCL, i.e. entirely terrestrial areas. The second part of discussion then presents an overall pattern of retreat for the study area linking the individual landform processes into a larger model.

4.1 Landform formation

4.1.1 De Geer Moraines

The ice front ran NE-SW with ice flow following the local topography. The far south of the study area was at deglaciation beneath 10-120 m of water in the west and east with a central highland ridge separating the two aquatic areas (Figs. 3A, 17). Water was up to 80 m-120 m deep across several kilometres of the ice margin, within the valleys seen in the study area today. The ice front in the west and east in these deep water areas was likely steep and grounded allowing the deposition of moraines. Calving bays formed and the ice margin underwent a stepwise retreat as is indicated by the regular pattern of distribution of the De Geer moraines below the HCL (Fig 4). Evidence of calving bay formation has been described across the SIS margin (Gillberg 1961; Strömberg 1981; Strömberg 1989; Lindén & Möller 2005; Dowling et al. 2016) and within Värmland (Lundqvist 1988). These bays act as major drainage outlets and can have the effect of thinning ice in surrounding areas and further back into the ice sheet itself (Benn et al. 2007). The hillshade models show De Geer moraines as distinct linear features all below the HCL (Fig. 4), however their prominence in the field is negligible. The position below the HCL in a deep water environment led to many of the moraines becoming buried beneath silt, sand and outwash material during and after deglaciation.

The formation of De Geer moraines in the study area was limited to the south east and south west where water depths were 80 m+ across several kilometres of the ice margin. The area below the HCL in the north-east also had deep water areas of up to 90 m but these were not as laterally extensive along the ice front as the deep water to the south. Valley sides shallowed quickly and the ice margin was grounded in mostly very shallow water. The buoyancy of the ice in the shallow water was not enough to lift large blocks and form De Geer moraines as in the model by Lindén & Möller (2005). This change in the deglaciation dynamics in this area, with the ice front sitting above a wide, shallow aquatic zone is similar to variations noted to the east of the study area by Lundqvist (2003). The nature of ice-retreat and break-up changed with retreat into shallow water and calving bays became much smaller or absent.

As the ice margin retreated further north, the western part of the study area became entirely terrestrial based whilst to the east the topography began to exert greater influence in a generally shallowing aquatic environment. Eskers formed in three adjacent valleys and the formation of De Geer moraines stopped completely suggesting a more irregular nature of general retreat and calving of a less uniform ice front.

4.1.2 Push Moraines

The moraines present in the north of the study area (Fig. 5) lie below the HCL in two wide, flat valleys. These areas lay beneath 10 m to 100 m of water at the time of deglaciation. Formation of the moraine ridges can be attributed to the presence of ice tongues/lobes within the valleys. Seasonal slight re-advance of these ice lobes during winter pushed sediment in front into ridges. The ice then retreated further in the following melt season and the moraine ridges remained behind further down the valley. The convex profile of the ridges in the north east sets (Fig. 5B) allows them to be distinguished from De Geer moraines that show a concave profile, reflecting the presence of a calving bay in the margin. The push moraines formed as the margin was becoming increasingly thinner and dominantly terrestrially based with aquatic terminating areas concentrated in valleys.

4.1.3 Tunnel Fill Eskers

The largest eskers present in the study area are located in prominent valleys following major structural lineations. These eskers run to many kilometres in length and are oriented NW-SE, oblique to the N-S ice flow direction as shown from orientation of streamlined features (Fig. 5), indicating that flow at the margin was topographically controlled. Deposition in the valley systems can be attributed to increasing topographical control on ice flow direction and sub-glacial drainage with thinning of the ice sheet. As such the major valleys became principal conduits for drainage of melt water and entrained material from beneath the ice sheet. Sub-glacial tunnels formed within the valleys and channelled water to the ice front. Deposition occurred within these tunnels and built eskers that were then exposed as the ice retreated. These eskers are identified in areas above and below the HCL. It is probable that NW-SE trending eskers were also deposited below the HCL in the base of the Rottnen and Rojdan river valleys and between De Geer moraines but were subsequently buried by fine silt and sands in deep water areas. The mode of deposition in tunnels in both aquatic and terrestrial settings is well established (Warren & Ashley 1994; Benn & Evans 2004).

4.1.4 Deltas

The two prominent deltas found within the study area (Fig. 9) occur along the HCL at the position where the margin was withdrawing from the aquatic environment and becoming terrestrially based (Fig. 17C). The for-

mation of deltas represents a period of slowed or stalled retreat of the ice margin as the delta formation takes time, also noted by Lundqvist (2003) in the neighbouring Klarälven Valley. The deltas in the study area both occur within the central highland area that is dominantly above the HCL. This positioning suggests that the rate of retreat of the terrestrially based margin slowed and became less regular compared to the stepwise retreat observed in the deep water areas marked by the regular formation of De Geer moraines.

4.1.5 Outwash plain and pitted outwash

The outwash plain at the end of the Rottnen river valley (Fig. 12) and the pitted outwash along the valley floor are evidence of a very high transport of sediment during deglaciation. This valley is unique in that a prominent esker is not identified unlike in all the neighbouring NW-SE trending valleys in the study area. If there exists an esker, it has likely been buried beneath the outwash sediments. This valley lies in the centre of the high-ground ridge that runs through the study area. It is bounded to the east and west by ridges up to 450 m in height and a wide bedrock plain lies to the west. The valley is incised ~200 m below the ridge and plain and acts as the prominent topographic low point and thus as a natural focus for drainage in the area. Topography acted to channel meltwater and entrained material into the valley where it was deposited rapidly and built up far above the contemporary water level. Much of the material flowed down the valley and was deposited above the HCL before it reached the base level to the south. Once the transport of sediment began to reduce, the river began to incise into its formerly deposited sediments, producing a series of erosional terraces and migrating channels that are evident in the hillshade models, and in the field (Fig. 15C). Land uplift due to isostatic rebound also resulted in incision as the river eroded down towards the base level.

4.1.6 Streamlined Terrain

The calving bays along the ice margin caused ice-thinning in the area lying to the north and nunataks likely began to appear. Ice over intervening high ground at the margin thinned and melted away with active ice becoming confined to valleys and lower ground. The thinning of ice over the most elevated areas during the retreat possibly acted to preserve streamlined landforms. At mid and low elevations there are no observable occurrences of streamlined features; either they were never formed in these areas or they are covered by later deposited sediments.

The ice flow direction close to the ice margin, ice surface profile and basal conditions altered with retreat across the study area. Streamlined terrain suggests a shift from a dominantly NNE-SSW ice-sheet flow direction in the south of the study area towards an N-S flow direction further north. The change in direction of streamlined features from NNE-SSW to N-S represents the start of a pivot of the ice front towards the higher elevations of central Sweden and the Scandes Mountains in Norway. Lundqvist (1992) noted the influence of two ice domes on ice flow and pattern of retreat. An ice dome over western Scandinavia was found to exert greater influence on western Värmland than a dome over the Gulf of Bothnia. The retreat around Torsby is moving towards the western Scandinavian dome and flow from the NE is of limited influence on the ice sheet in this area at this stage. This fits the larger scale model of Stroeven et al. (2015). Underlying bedrock topography also began to exert a greater influence with the thinning and break-up of the ice sheet. The regional major faults of the mylonite formation all trend NW-SE and present within the landscape as major valleys, often deepening to 200 m+.

The flow direction indicated by the streamlined features is thus different to the NW-SE flow closer to the retreating margin, as indicated by the orientation of eskers and De Geer moraines identified in the study area. This is probably due to that the streamlined features formed further from the margin in areas of thicker ice where topographic control on ice movement was less. A similar adjustment in ice flow direction with proximity to the margin was observed by Dowling et al. (2016) on the Närke Plain in south-central Sweden.

4.1.7 Transverse Eskers

The sinuous, sand rich transverse eskers in the north of the study area are suggested to have formed within crevasses in frontally stagnated ice. The area in which they formed is noticeable for being a flat plain surrounded on three sides by high relief and bisected by the HCL. This plain is now covered by hummocky terrain indicating that deposition from stagnating and dead ice melt out was a prominent process in this area. The process of esker deposition in ice walled channels transverse to ice flow is noted by Benn & Evans (2004) and Johansson (1994). The eskers also lie right on the margin of the 190 m HCL limit. These features likely formed during the final stages of deglaciation within the area. An ice lobe extended onto the plain (Fig 17F) and was fed by two outlets from the ice sheet, one within the Rottnen valley to the NW and another through a smaller valley directly north of the latter (Fig 17F). This lobe probably became stagnant and detached, in a later stage, from active ice. To cover the plain the ice lobe would have had an area of at least 20 km^2.

The ice that lay below the HCL decayed quickly, evidenced by fewer hummocks and poorer preservation of relict streamlined features to the east. The western section of the lobe decayed slowly with a steady low flow of meltwater and finer grained material draining through crevasses. Material aggraded within these ice walled channels as evidenced by section S03 (Fig 10). The ice remained for a prolonged period allowing the deposits to stabilise with a steep, sharp crested profile. Final melt-out of surrounding ice deposited the upper most gravels that cover the deposits and also the hummocks that lie adjacent to and over parts of the northern most transverse esker. The distinct sinuous profile of the eskers shows the control over deposition of the glacier structure. The path of the esker reflects the shape of the crevasse in which it was deposited. This was also noted by Evans & Twigg (2002).

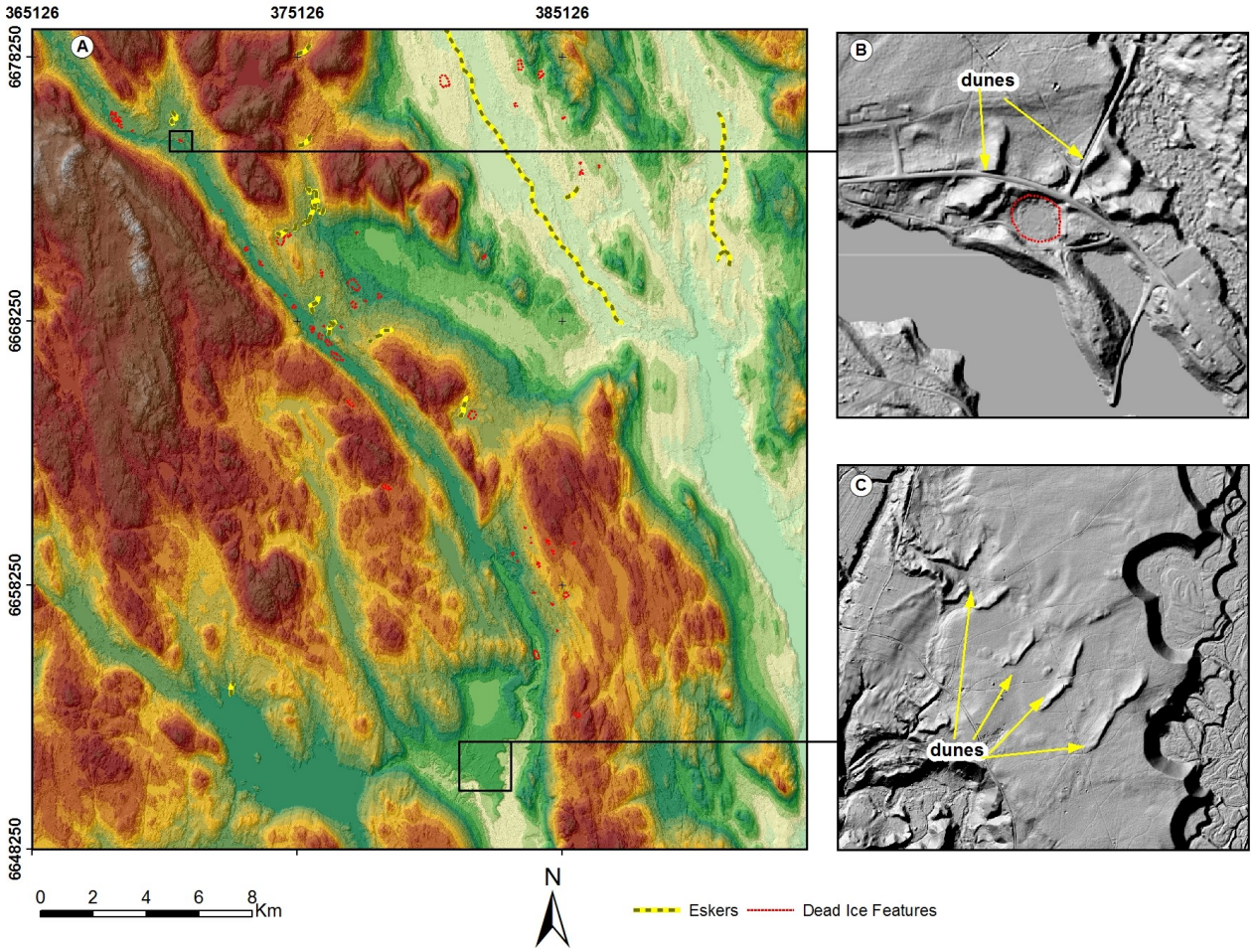

Fig. 15. Dune sets identified in study area on outwash plains. Dunes in (B) and (C) have concave planform profiles indicating dominant wind direction from the NW. Dunes in (C) may reflect morphology of underlying glaciofluvial or geological features. Hillshade generated from LiDAR scan data provided by Lantmäteriet, Sweden © Lantmäteriet, i2012/927.

4.1.8 Hummocky Terrain

Hummocky terrain is most common in the north of the study area in lowland areas. Smaller areas are found across the highland to the north-west. In these high areas ice-melting was the source of englacial material being deposited into dead ice depressions or depressions over already deglaciated ground. Gradual melting of ice also produced lakes in which fine grained sands and silt were deposited. The largest areas of hummocky terrain are found across the low ground in the north and north-east of the study area in zones around the HCL. Stagnant ice blocks likely remained in these areas once the main ice sheet had retreated. As they melted the hummocky terrain visible today formed in the manner put forward by Möller & Dowling (2015) with final melting of ice blocks producing the kettle holes and small ponds and lakes present across the area. Deposition of supraglacial material from ice in the north east (Fig 14) into shallow water could have created a debris covered area below the HCL.

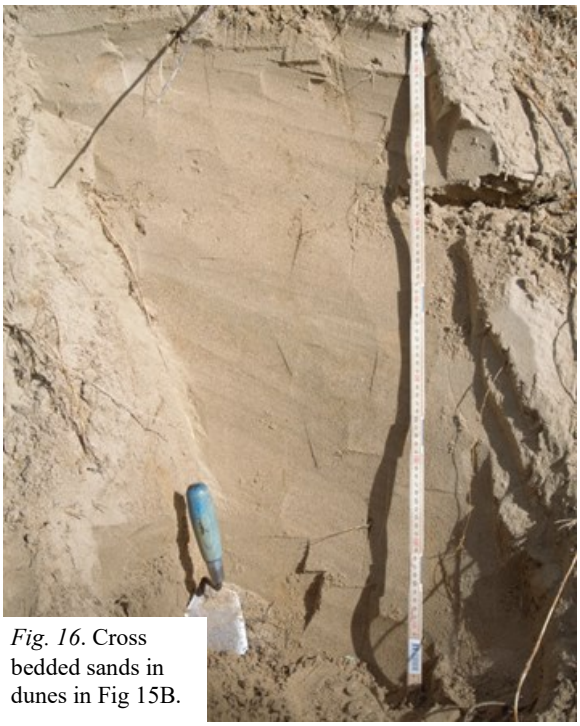

Fig. 16. Cross bedded sands in dunes in Fig 15B.

4.1.9 Dunes

The two dune sets (Fig. 15B and C) are evidence of

post-glacial aeolian processes. Formation likely started immediately following deglaciation. Fine sands and sediments not yet extensively vegetated in areas above the HCL were wind eroded, transported, and eventually deposited as dunes, predominantly transverse to prevailing wind direction. It is also possible that the dunes further developed during more recent periods of wind deflation as e.g. noted in the dune fields at Brattforsheden to the south east of the study area (Alexanderson & Fabel 2015).

4.2 Pattern of Retreat

The features identified in the study area present a pattern of transition from aquatic to terrestrial conditions as the margin retreated to the NW. This also highlights how the process of deglaciation and ice-loss alters with this change. Studies of the British Ice Sheet (Clark et al. 2012), the Barents Sea Ice Sheet (Winsborrow et al. 2010) and the Greenland Ice Sheet (Warren & Hulton 1990) have all suggested a clear reduction in retreat rates and increasing topographic control on ice sheet movement with transition from an aquatic to terrestrial margin. This change is attributed to the ice sheets adjusting to the loss of calving bays as an outlet and site of ice loss. The influence of underlying topography is clearly evident in the study area with the differing orientation between streamlined terrain, which formed more distal from the margin, and marginal glacial features that formed beneath thinner ice towards the ice margin or at the margin proper. An overview of the ice sheet retreat across the study area is presented below and summarised map-wise in six time steps (Fig. 17, A-F). This model is based on geological features identified within this study and reasoned interpolation between them. The margin below the HCL was defined by following the orientation of De Geer moraines. Deltas and areas of outwash accumulation determined points where the ice sheet slowed its retreat whilst eskers and drainage channels helped define position of ice within valleys. Kettle holes guided placement of dead ice areas alongside hummocky terrain. Inferred earlier exposure of the greatest elevations is drawn from drainage channels and sediment accumulations at the foot of exposed, weathered rocky ridges and outcrops and likely drawdown of ice over elevated areas as the ice sheet thinned close to the margin.

Initially the entire study area was covered by the SIS with all but the central part of the ice-sheet over the high-ground ridge terminating in the Yoldia Sea/Vänern Basin (Fig. 17A) (Björck 1995). Calving bays were present along a steep ice front to the west and east with the ice sheet grounded in the aquatic zone. Icebergs calved away from the ice face and buoyancy contrasts induced large blocks to break off from below the waterline (Lindén & Möller 2005). The retreat in this manner is marked by the deposition of multiple De Geer moraines across the extent of the aquatic margin area (Fig. 4). The rapid outflow through calving bays caused a thinning of ice within the ice sheet, particularly over high-ground areas proximal to the margin. The terrestrially based ice along the central ridge thinned and nunataks began to appear (Fig. 17 A-B). As the ice receded over the high-ground above the HCL it became stagnant and decayed, leaving ice behind within bedrock hollows and also along valleys. Small eskers formed within valleys where larger ice volumes persisted and possibly remained active for a period beyond the main ice sheet retreat. The ice margin was oriented WSW-ENE with an ice flow direction at the margin perpendicular to this. The flow of ice further behind the margin, where the ice remained thicker, was from the NNE.

With continued ice margin retreat towards the NNW, calving bays continued to channel ice away from the ice-sheet margin but became less widespread as more of it retreated into shallow water or became entirely terrestrially based. Ice flow became more influenced and constrained within major valleys following the NW-SE trending faults, and between peninsulas that were now protruding into the sea (Fig. 17B).

The ice sheet began a transition to terrestrial frontal conditions in the west and the aquatic extent of the margin narrowed in the east (Fig 17C). Fewer calving bays were active and those that remained were situated between islands and peninsulas. With the transition to dominantly terrestrial conditions the pace of retreat slowed and pattern of deglaciation began to alter. Thinning of ice over high ground areas continued and large volumes of melt-water were channelled to the ice front along the major NW-SE trending valleys. The ice sheet retreat slowed markedly at the area of aquatic-terrestrial transition and deltas were able to build as sediment carried within meltwater was deposited in deeper water at the ice-margin.

Topographical influence on ice flow increased and areas of active ice at the terrestrial margin became confined to valleys (Fig. 17D). Calving bays continued to shut down and deposition of De Geer moraines became more sporadic and of a smaller size. Dead ice blocks persisted in lower elevation areas. The ice sheet continued to thin over high elevations with the Rottnen Valley now acting as the main drainage conduit for the terrestrial part of the ice sheet in the study area. A large delta became established at the end of the valley and was also fed by a smaller, ice tongue to the west.

As the ice-sheet retreated to northwest-wards it became entirely terrestrially based in the west and sat in a wide, dominantly shallow (<40 m) aquatic zone to the east (Fig. 17E). The pattern of regular calving and retreat stopped. Ice thinned rapidly over higher elevations. A thick outwash sequence began to build in the Rottnen Valley. Topographical control on ice flow increased further and drainage was focussed along valleys following the NW-SE regional structures. Eskers were deposited within these valleys and dead ice was left, being the source for formation of kettle holes and hummocky terrain.

The ice-sheet had thinned markedly by the time the margin retreated to the north of the study area (Fig. 17F). Active ice was concentrated to flow within and directed by valleys in both the terrestrial and aquatic areas. Ice lobes formed across lowland areas at the heads and sides of valleys. The margin of these lobes was marked by the formation of small push moraines. These lobes eventually became stagnant and separated

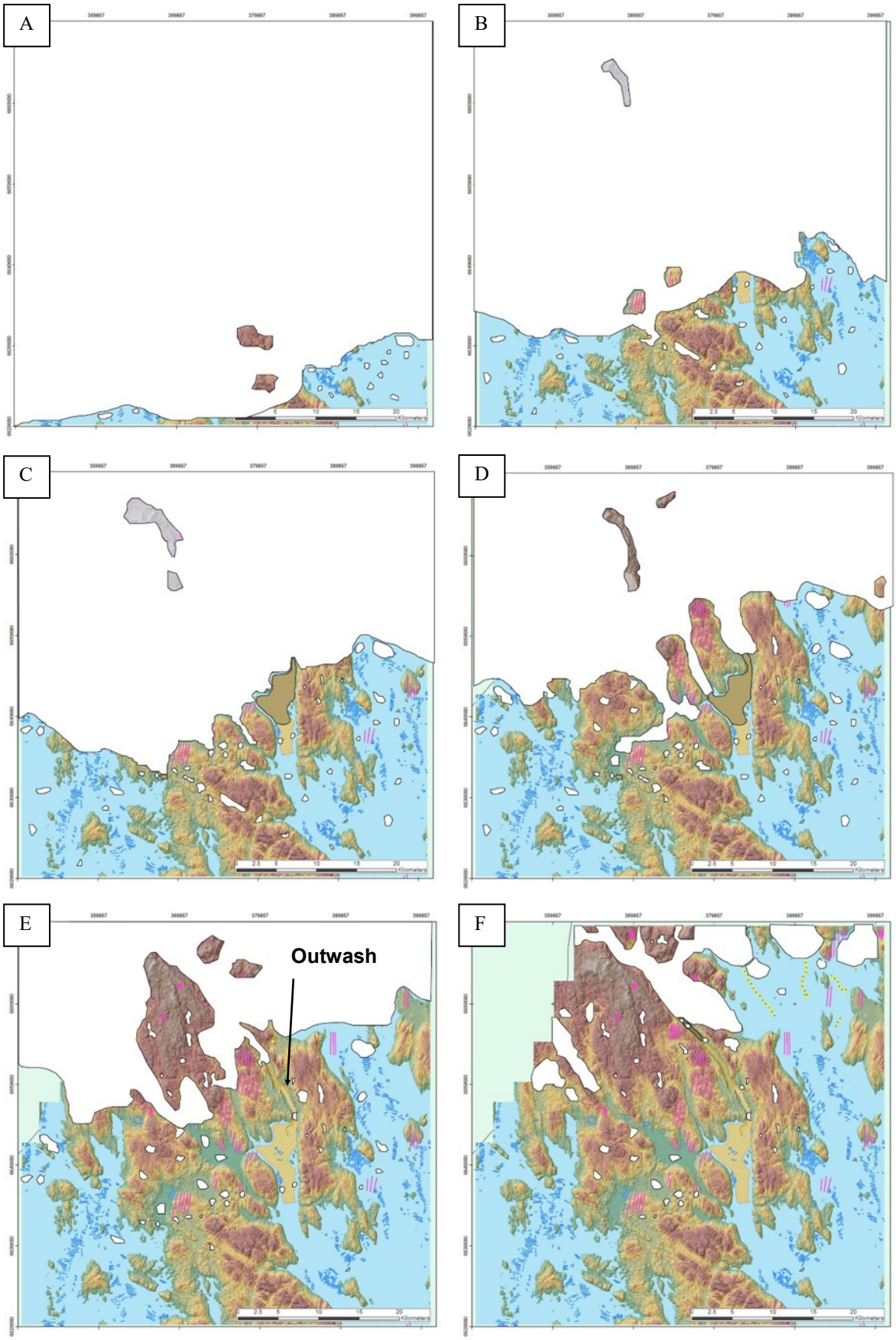

Fig . 17. Proposed model of ice sheet retreat and decay across study area. The retreat in this area is estimated to have taken place over c.200 years. Hillshade generated from LiDAR scan data provided by Lantmäteriet, Sweden © Lantmäteriet, i2012/927.

from active ice and began to decay. The decay of these lobes resulted in the formation of large areas of hummocky terrain. The transverse eskers identified in this study also formed at this time as the lobe on the eastern side of the Rottnen Valley melted.

Finally active ice retreated from the entire study area. However, dead-ice blocks remained along valleys and continuing fluvial action and deposition of outwash material from further north acted to form terraces and built deposits around dead ice blocks that would eventually form kettle holes. A similar pattern was found by Lundqvist (2003) in the Klarälven Valley adjacent to the study area to the east. The initial retreat of the margin on-land caused a slowing of retreat but this was likely short lived as the ice that had thinned was predisposed to melting as noted by Clark et al. (2012) in their study of the British Ice Sheet. As the ice margin became increasingly distal to the study area the volume of meltwater and entrained sediment decreased and streams and rivers began to incise into the outwash plains and terraces. Land uplift due to isostatic rebound and lowering of the base level also induced incision. Dunes then began to form due to aeolian activity on outwash plains as re-working by fluvial action ceased and water content decreased.

4.3 Chronology of retreat

An accurate chronology of retreat is not within the scope of this investigation and accurate dating of features and materials from the study area is lacking. However, there are several relevant studies that allow a rudimentary outline of timing of the ice-recession across the study area. The pattern of rapid aquatic retreat followed by slowed terrestrial is well established in south and central Sweden (Boulton et al. 2001; Stroeven et al. 2015). Timing and stages of the Baltic Sea and its extension into the Lake Vänern basin were set out by Björck (1995) who placed the aquatic period studied here within the late Yoldia Sea stage, c. 10.5 cal ka BP. The pace and dynamics of retreat in Värmland have been studied in most detail by Lundqvist (1988, 1992, 2003). The study of the deglaciation pattern along the Klarälven Valley by Lundqvist (2003) is of particular relevance as this valley lies only ~20 km to the east of the study area and also follows the same major NW-SE fault set.

Projection of the ice front between the two areas, correlation with depositional features identified in this study and the time-scale established for retreat in the Klarälven Valley allows for a basic comparative chronology to be developed. The south of the study area lies along the assumed margin from Lake Grässjön in the Klarälven Valley. Both areas show a transition from a wide ice front situated on plains below the HCL to active ice becoming concentrated in valleys with thinning over high ground. Time of retreat at Lake Grässjön is set at 10.75 cal ka BP. The northern extension of the study area lies along the assumed margin from the confluence of the Hälgån River and the Klarälven. The margin is placed at this site at 10.5 cal ka BP and is represented by a marginal delta. This rough correlation suggests the ice margin retreated across the study area over ~186 years with an annual retreat of the main margin of ~215 m per year across the central 40 km of the study area. This fits with the retreat rate suggested by Stroeven et al. (2015), determined across southern and central Sweden following the Younger Dryas. As previously stated the retreat rate would have varied depending on prevailing aquatic or terrestrial conditions at the margin. Also the behaviour of a glacier in one valley can often differ markedly from one in a neighbouring valley.

5. Conclusions

Analysis of LiDAR data and field investigations have revealed a distinct pattern of retreat of the Scandinavian Ice Sheet across the study area. A clear transitional zone exists with the ice sheet withdrawing from the Yoldia Sea/Vänern Basin into a terrestrial setting. This zone is recognised through the presence of characteristic sub-aquatic, sub-glacial and pro-glacial features.

The ice sheet margin was initially aquatic terminating across the whole area except for a central ridge of elevated land. Calving bays drove rapid retreat and caused thinning of the ice sheet over the elevated areas, resulting in concentration of active ice within valleys and lowland. With retreat northwards the western side of the margin withdrew on land and the aquatic terminating area of the eastern margin narrowed and withdrew into shallower water. The retreat slowed for a period when the margin reached the highest coastline and deltas formed. Thinning of ice over high-ground continued and active ice became further concentrated in valleys. Outwash plains established beyond the ice margin in the Rottnen valley and dead ice became isolated and buried. Topographic control on ice flow became more pronounced with retreat north-west-wards and active ice took the form of outlet tongues spurring off the main ice sheet. An ice lobe became isolated on the east of the Rottnen Valley and decayed, resulting in the formation of transverse eskers within crevasses and hummocky terrain in the surrounding area.

Rough dating of the retreat via correlation with previous studies places it at between 10.75 cal ka BP and 10.55 cal ka BP with an average retreat rate of ~215 m per year.

This study shows that combined analysis of detailed remote sensing data and targeted field investigations can quickly establish a pattern of ice-margin retreat at decadal to centennial scale. With the current requirement to better understand ice-sheet retreat on human time-scales becoming ever more pressing, this combination of data allows more detail to be rapidly introduced to models of ice-sheet behaviour. The dynamics of extant ice-sheets may still not be fully understood but they share many of the same conditions as experienced by now extinct sheets. Though we were not able to witness the decay of the SIS and its contemporaries they left their mark and with more detailed observations of formerly glaciated areas the shorter term behaviour of these ice sheets is becoming clearer and applicable to the present day.

5.1 Further Work

There are two principle areas where further work could be focussed.

Within the study area itself there remain a number of features worthy of more detailed investigation such as further sedimentological investigation of the marginal deltas, closely spaced De-Geer moraines and transverse eskers, to name a few. Of particular use would be cosmogenic dating of elevated bedrock areas to better constrain the date of exposure during deglaciation. The aim of this investigation was to see if LiDAR and field analysis could reveal a more detailed pattern of deglaciation over a shorter time-scale. This has been achieved but further detail may still be added through study of the features on the ground.

The clear transitional zone revealed should be able to be traced along the ice margin around the HCL. It would be of great interest to observe if the same pattern of changing landforms is common along the margin or if the transition is marked in differing ways. Also evidence of extremely rapid retreat and possible localised re-advances would add a further dimension to knowledge of the dynamics of the margins retreat.

6 Acknowledgements

Massive thanks to Helena Alexanderson for helping decide the theme of this thesis and giving plenty of invaluable feedback and advice along the way. Also many thanks to Per Möller for feedback and comments to improve the focus and presentation of this paper.

7 References

Alexanderson, H. & Fabel, D., 2015: Holocene Chronology of the Brattforsheden Delta and Inland Dune Field, Sweden. *Geochronometria: 42, 1 -16*. doi: 10.1515/geochr-2015-0001

Alexanderson, H. & Murray, A. S., 2012: Problems and potential of OSL dating Weichselian and Holocene sediments in Sweden. *Quaternary Science Reviews 44*, 37-50.

Andersen, B. G., Lundqvist, J. & Saarnisto, M., 1995a: The Younger Dryas Margin of the Scandinavian Ice Sheet. *Quaternary International 28*, 145.

Andersen, B. G., Mangerud, J., Sørensen, R., Reite, A., Sveian, H., Thoresen, M. & Bergström, B., 1995b: Younger Dryas ice-marginal deposits in Norway. *Quaternary International 28*, 147-169. doi: http://dx.doi.org/10.1016/1040-6182(95)00037-J

Balco, G., 2011: Contributions and unrealized potential contributions of cosmogenic-nuclide exposure dating to glacier chronology, 1990–2010. *Quaternary Science Reviews 30*, 3-27.

Banerjee, D., Murray, A. S., Bøtter-Jensen, L. & Lang, A., 2001: Equivalent dose estimation using a single aliquot of polymineral fine grains. *Radiation Measurements 33*, 73-94.

Benn, D. I. & Evans, D. J. A., 2004: *Glaciers and Glaciation*. Routledge.

Benn, D. I., Warren, C. R. & Mottram, R. H., 2007: Calving processes and the dynamics of calving glaciers. *Earth-Science Reviews 82*, 143-179.

Bennett, M. R., 2001: The morphology, structural evolution and significance of push moraines. *Earth Science Reviews 53*, 197-236. doi: 10.1016/S0012-8252(00)00039-8

Björck, S., 1995: A review of the history of the Baltic Sea, 13.0-8.0 ka BP. *Quaternary International 27*, 19-40. doi: http://dx.doi.org/10.1016/1040-6182(94)00057-C

Boone, S. & Eyles, N., 2001: Geotechnical model for great plains hummocky moraine formed by till deformation below stagnant ice. *Geomorphology 38*, 109-124.

Böse, M., Lüthgens, C., Lee, J. R. & Rose, J., 2012: Quaternary glaciations of northern Europe. *Quaternary Science Reviews 44*, 1-25.

Boulton, G. S., Dongelmans, P., Punkari, M. & Broadgate, M., 2001: Palaeoglaciology of an ice sheet through a glacial cycle:. the European ice sheet through the Weichselian. *Quaternary Science Reviews 20*, 591-625. doi: 10.1016/S0277-3791(00)00160-8

Bouvier, V., Johnson, M. D. & Påsse, T., 2015: Distribution, genesis and annual-origin of De Geer moraines in Sweden: insights revealed by LiDAR. *GFF 137*, 319-333.

Brennand, T. A., 2000: Deglacial meltwater drainage and glaciodynamics: inferences from Laurentide eskers, Canada. *Geomorphology 32*, 263-293. doi: http://dx.doi.org/10.1016/S0169-555X(99)00100-2

Clark, C. D., Hughes, A. L. C., Greenwood, S. L., Jordan, C. & Sejrup, H. P., 2012: Pattern and timing of retreat of the last British-Irish ice sheet. *Quaternary Science Reviews 44*, 112-146. doi: 10.1016/j.quascirev.2010.07.019

Clark, P. U., Dyke, A. S., Shakun, J. D., Carlson, A. E., Clark, J., Wohlfarth, B., Mitrovica, J. X., Hostetler, S. W. & Mccabe, A. M., 2009: The last glacial maximum. *Science 325*, 710-714.

Dowling, T. P., Alexanderson, H. & Möller, P., 2013: The new high-resolution LiDAR digital height model ('Ny Nationell Höjdmodell') and its application to Swedish Quaternary geomorphology. *GFF 135*, 145-151.

Dowling, T. P., Möller, P. & Spagnolo, M., 2016: Rapid subglacial streamlined bedform formation at a calving bay margin. *Journal of Quaternary Science 31*, 879-892.

Duller, G. A., 2004: Luminescence dating of Quaternary sediments: recent advances. *Journal of Quaternary Science 19*, 183-192.

Evans, D. J. A. & Twigg, D. R., 2002: The active temperate glacial landsystem: a model based on Breiðamerkurjökull and Fjallsjökull, Iceland. *Quaternary Science Reviews 21*, 2143-2177. doi: http://dx.doi.org/10.1016/S0277-3791(02)00019-7

Evans, J. S., Hudak, A. T., Faux, R. & Smith, A., 2009: Discrete return lidar in natural resources: Recommendations for project planning, data processing, and deliverables. *Remote Sensing 1*, 776-794.

Eyles, N., Boyce, J. I. & Barendregt, R. W., 1999: Hummocky moraine: sedimentary record of stagnant Laurentide Ice Sheet lobes resting on soft beds. *Sedimentary Geology 123*, 163-174.

Gillberg, G., 1961: The Middle-Swedish moraines in the province of Dalsland, W Sweden. *GFF 83*, 335-369.

Johansson, P., 1994: The subglacially engorged eskers in the Lutto river basin, northeastern Finnish Lapland. *Formation and deformation of glacial deposits*, 89-94.

Johansson, P., Lunkka, J. P. & Sarala, P. 2011: Chapter 9 - The Glaciation of Finland. *In* J. Ehlers, P. L. Gibbard & D. H. Philip (eds.): *Developments in Quaternary Sciences*, 105-116. Elsevier,

Johnson, M. D., Fredin, O., Ojala, A. E. & Peterson, G., 2015: Unraveling Scandinavian geomorphology: the LiDAR revolution. *GFF 137*, 245-251.

Lindén, M. & Möller, P., 2005: Marginal formation of De Geer moraines and their implications to the dynamics of grounding-line recession. *Journal of Quaternary Science 20*, 113.

Lønne, I., 1995: Sedimentary facies and depositional architecture of ice-contact glaciomarine systems. *Sedimentary Geology 98*, 13-43.

Lundqvist, J., 1958: Beskrivning till jordartskarta över Värmlands län. *Sveriges geologiska undersökning CA 38*.

Lundqvist, J., 1988: Younger Dryas-Preboreal moraines and deglaciation in southwestern Värmland, Sweden. *Boreas 17*, 301-316.

Lundqvist, J., 1992: Moraines and Late Glacial Activity in Southern Värmland, Southwestern Sweden. *Geografiska Annaler. Series A, Physcial Geography.* Swedish Society for Anthropology and Geography. 245 pp.

Lundqvist, J., 1995: The Younger Dryas Ice-Marginal Zone in Sweden. *Quaternary International 28*, 171-176. doi: http://dx.doi.org/10.1016/1040-6182(95)00032-E

Lundqvist, J., 2003: Deglaciation pattern in sub-aquatic—supra-aquatic transitional environment illustrated by the Klarälven valley system, Värmland, western Sweden. *Geografiska Annaler: Series A, Physical Geography 85*, 73-89.

Mcclenaghan, M. B., 2001: Drift exploration in glaciated terrain. Geological Society of London.

Möller, P. & Dowling, T. P. F., 2015: The importance of thermal boundary transitions on glacial geomorphology; mapping of ribbed/hummocky moraine and streamlined terrain from LiDAR, over Småland, South Sweden. *GFF 137*, 252-283. doi: 10.1080/11035897.2015.1051736

Murray, A. S. & Wintle, A. G., 2000: Luminescence dating of quartz using an improved single-aliquot regenerative-dose protocol. *Radiation Measurements 32*, 57-73.

Murray, A. S. & Wintle, A. G., 2003: The single aliquot regenerative dose protocol: potential for improvements in reliability. *Radiation Measurements 37*, 377-381.

Peterson, G. & Smith, C. A., 2013: Description of units in the geomorphic database of Sweden. *SGU-Rapport 4*, 18.

Rees, G. & Rees, W. G., 2013: *Physical principles of remote sensing*. Cambridge University Press.

Roberts, H. M., Durcan, J. A. & Duller, G. a. T., 2009: Exploring procedures for the rapid assessment of optically stimulated luminescence range-finder ages. *Radiation Measurements 44*, 582-587. doi: 10.1016/j.radmeas.2009.02.006

Saarnisto, M. & Saarinen, T., 2001: Deglaciation chronology of the Scandinavian Ice Sheet from the Lake Onega Basin to the Salpausselkä End Moraines. *Global and Planetary Change 31*, 387-405. doi: 10.1016/S0921-8181(01)00131-X

SGU, 2016: Lantmäteriet Laserdata 2016. Retrieved 2016, from https://maps.slu.se/

Smith, M. J. & Clark, C. D., 2005: Methods for the visualization of digital elevation models for landform mapping. *Earth Surface Processes and Landforms 30*, 885-900. doi: 10.1002/esp.1210

Solheim, A., 1983: Quatemary sediments and bedrock geology in the outer Oslofjord and northemmost Skagerrak. *Norsk Geologisk Tidsskrift 63*, 55-72.

Stanton, T., Snowball, I., Zillén, L. & Wastegård, S., 2010: Validating a Swedish varve chronology using radiocarbon, palaeomagnetic secular variation, lead pollution history and statistical correlation. *Quaternary Geochronology 5*, 611-624.

Stroeven, A. P., Hättestrand, C., Kleman, J., Heyman, J., Fabel, D., Fredin, O., Goodfellow, B. W., Harbor, J. M., Jansen, J. D., Olsen, L., Caffee, M. W., Fink, D., Lundqvist, J., Rosqvist, G. C., Strömberg, B. & Jansson, K. N., 2015: Deglaciation of Fennoscandia. *Quaternary Science Reviews*. doi: http://dx.doi.org/10.1016/j.quascirev.2015.09.016

Strömberg, B., 1981: Calving bays, striae and moraines at Gysinge-Hedesunda, central Sweden. *Geografiska Annaler. Series A. Physical Geography*, 149-154.

Strömberg, B., 1989: Late Weichselian deglaciation and clay varve chronology in east-central Sweden. *Sveriges geologiska undersökning. Serie Ca. Avhandlingar och uppsatser I 4: 0*, 3-70.

Sugden, D. E. & John, B. S., 1976: *Glaciers and landscape*. E. Arnold.

Truffer, M. & Fahnestock, M., 2007: Rethinking Ice Sheet Time Scales. *Science* 315. 1508-1510.

Vaughan, D. G. & Arthern, R., 2007: Why is it hard to predict the future of ice sheets? *Science (Washington) 315*, 1503-1504.

Warren, C. & Hulton, N., 1990: Topographic and glaciological controls on Holocene ice-sheet margin dynamics, central West Greenland. *Annals of Glaciology 14*, 307-310.

Warren, W. P. & Ashley, G. M., 1994: Origins of the ice-contact stratified ridges (eskers) of Ireland. *Journal of Sedimentary Research 64*.

Winsborrow, M. C. M., Andreassen, K., Corner, G. D. & Laberg, J. S., 2010: Deglaciation of a marine-based ice sheet: Late Weichselian palaeo-ice dynamics and retreat in the southern Barents Sea reconstructed from onshore and offshore glacial geomorphology. *Quaternary Science Reviews 29*, 424-442. doi: http://dx.doi.org/10.1016/j.quascirev.2009.10.001

Zillén, L., Snowball, I., Sandgren, P. & Stanton, T., 2003: Occurrence of varved lake sediment sequences in Varmland, west central Sweden: lake characteristics, varve chronology and AMS radiocarbon dating. *Boreas 32*, 612-626.

Zillén, L. M., Wastegård, S. & Snowball, I. F., 2002: Calendar year ages of three mid-Holocene tephra layers identified in varved lake sediments in west central Sweden. *Quaternary Science Reviews 21*, 1583-1591.

Appendix

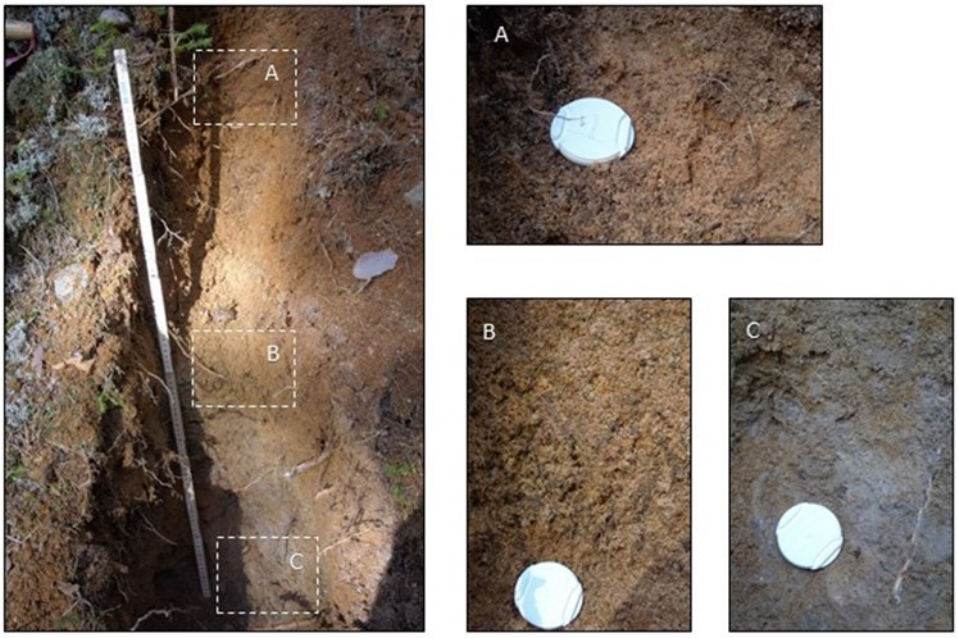

S01 Section

S02 Section

S03 Section

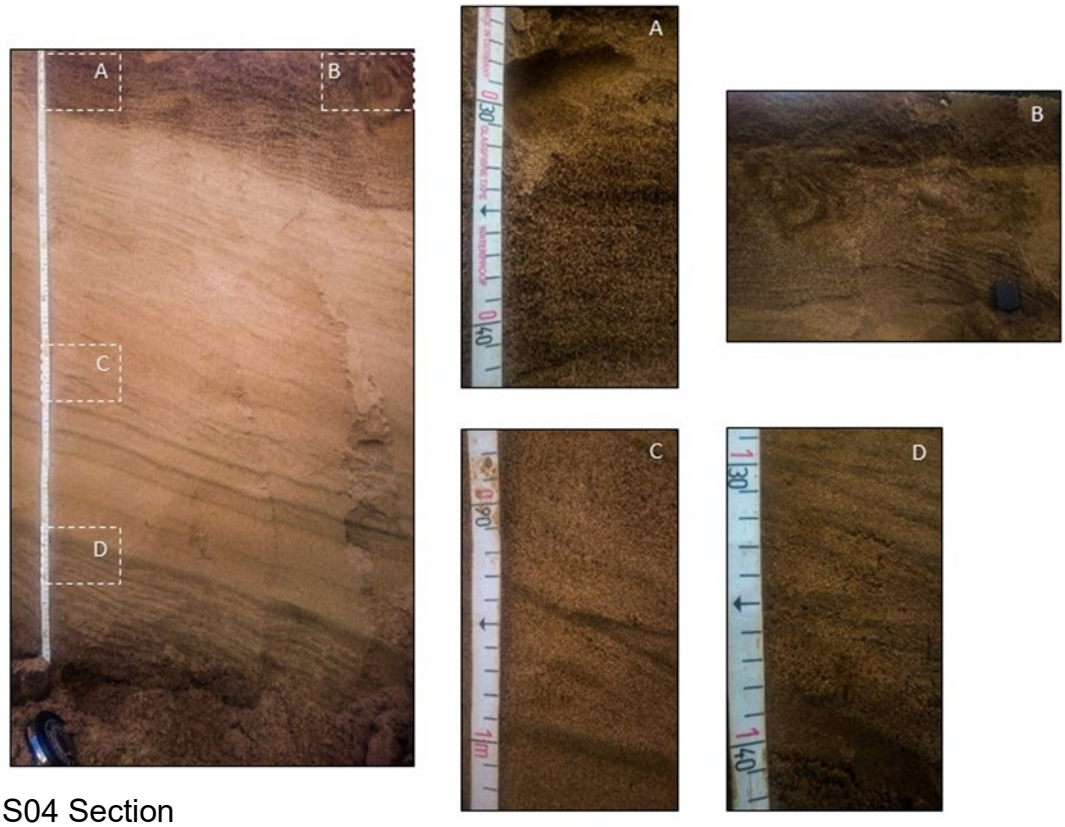

S04 Section

Tidigare skrifter i serien ”Examensarbeten i Geologi vid Lunds universitet”:

449. Nordas, Johan, 2015: A palynological study across the Ordovician Kinnekulle. (15 hp)
450. Åhlén, Alexandra, 2015: Carbonatites at the Alnö complex, Sweden and along the East African Rift: a literature review. (15 hp)
451. Andersson, Klara, 2015: Undersökning av slugtestsmetodik. (15 hp)
452. Ivarsson, Filip, 2015: Hur bildades Bushveldkomplexet? (15 hp)
453. Glommé, Alexandra, 2015: $^{87}Sr/^{86}Sr$ in plagioclase, evidence for a crustal origin of the Hakefjorden Complex, SW Sweden. (45 hp)
454. Kullberg, Sara, 2015: Using Fe-Ti oxides and trace element analysis to determine crystallization sequence of an anorthosite-norite intrusion, Älgön SW Sweden. (45 hp)
455. Gustafsson, Jon, 2015: När började plattektoniken? Bevis för plattektoniska processer i geologisk tid. (15 hp)
456. Bergqvist, Martina, 2015: Kan Ölands grundvatten öka vid en uppdämning av de utgrävda dikena genom strandvallarna på Ölands östkust? (15 hp)
457. Larsson, Emilie, 2015: U-Pb baddeleyite dating of intrusions in the south-easternmost Kaapvaal Craton (South Africa): revealing multiple events of dyke emplacement. (45 hp)
458. Zaman, Patrik, 2015: LiDAR mapping of presumed rock-cored drumlins in the Lake Åsnen area, Småland, South Sweden. (15 hp)
459. Aguilera Pradenas, Ariam, 2015: The formation mechanisms of Polycrystalline diamonds: diamondites and carbonados. (15 hp)
460. Viehweger, Bernhard, 2015: Sources and effects of short-term environmental changes in Gullmar Fjord, Sweden, inferred from the composition of sedimentary organic matter. (45 hp)
461. Bokhari Friberg, Yasmin, 2015: The paleoceanography of Kattegat during the last deglaciation from benthic foraminiferal stable isotopes. (45 hp)
462. Lundberg, Frans, 2016: Cambrian stratigraphy and depositional dynamics based on the Tomten-1 drill core, Falbygden, Västergötland, Sweden. (45 hp)
463. Flindt, Anne-Cécile, 2016: A pre-LGM sandur deposit at Fiskarheden, NW Dalarna - sedimentology and glaciotectonic deformation. (45 hp)
464. Karlatou-Charalampopoulou, Artemis, 2016: Vegetation responses to Late Glacial climate shifts as reflected in a high resolution pollen record from Blekinge, south-eastern Sweden, compared with responses of other climate proxies. (45 hp)
465. Hajny, Casandra, 2016: Sedimentological study of the Jurassic and Cretaceous sequence in the Revinge-1 core, Scania. (45 hp)
466. Linders, Wictor, 2016: U-Pb geochronology and geochemistry of host rocks to the Bastnäs-type REE mineralization in the Riddarhyttan area, west central Berglsagen, Sweden. (45 hp)
467. Olsson, Andreas, 2016: Metamorphic record of monazite in aluminous migmatitic gneisses at Stensjöstrand, Sveconorwegian orogen. (45 hp)
468. Liesirova, Tina, 2016: Oxygen and its impact on nitrification rates in aquatic sediments. (15 hp)
469. Perneby Molin, Susanna, 2016: Embryologi och tidig ontogeni hos mesozoiska fisködlor (Ichthyopterygia). (15 hp)
470. Benavides Höglund, Nikolas, 2016: Digitization and interpretation of vintage 2D seismic reflection data from Hanö Bay, Sweden. (15 hp)
471. Malmgren, Johan, 2016: De mellankambriska oelandicuslagren på Öland - stratigrafi och faciestyper. (15 hp)
472. Fouskopoulos Larsson, Anna, 2016: XRF -studie av sedimentära borrkärnor - en metodikstudie av programvarorna Q-spec och Tray-sum. (15 hp)
473. Jansson, Robin, 2016: Är ERT och Tidsdomän IP potentiella karteringsverktyg inom miljögeologi? (15 hp)
474. Heger, Katja, 2016: Makrofossilanalys av sediment från det tidig-holocena undervattenslandskapet vid Haväng, östra Skåne. (15 hp)
475. Swierz, Pia, 2016: Utvärdering av vattenkemisk data från Borgholm kommun och dess relation till geologiska förhållanden och markanvändning. (15 hp)
476. Mårdh, Joakim, 2016: WalkTEM-undersökning vid Revingehed provpumpningsanläggning. (15 hp)

477. Rydberg, Elaine, 2016: Gummigranulat - En litteraturstudie över miljö- och hälsopåverkan vid användandet av gummigranulat. (15 hp)
478. Björnfors, Mark, 2016: Kusterosion och äldre kustdyners morfologi i Skälderviken. (15 hp)
479. Ringholm, Martin, 2016: Klimatutlöst matbrist i tidiga medeltida Europa, en jämförande studie mellan historiska dokument och paleoklimatarkiv. (15 hp)
480. Teilmann, Kim, 2016: Paleomagnetic dating of a mysterious lake record from the Kerguelen archipelago by matching to paleomagnetic field models. (15 hp)
481. Schönström, Jonas, 2016: Resistivitets- och markradarmätning i Ängelholmsområdet - undersökning av korrosiva markstrukturer kring vattenledningar. (15 hp)
482. Martell, Josefin, 2016: A study of shock-metamorphic features in zircon from the Siljan impact structure, Sweden. (15 hp)
483. Rosvall, Markus, 2016: Spår av himlakroppskollisioner - bergarter i nedslagskratrar med fokus på Mien, Småland. (15 hp)
484. Olausson, My, 2016: Resistivitets- och IP -mätningar på den nedlagda deponin Gustavsfält i Halmstad. (30 hp)
485. Plan, Anders, 2016: Markradar- och resistivitetsmätningar – undersökningar utav korrosionsförhöjande markegenskaper kring fjärrvärmeledningar i Ängelholm. (15 hp)
486. Jennerheim, Jessica, 2016: Evaluation of methods to characterise the geochemistry of limestone and its fracturing in connection to heating. (45 hp)
487. Olsson, Pontus, 2016: Ekologiskt vatten från Lilla Klåveröd: en riskinventering för skydd av grundvatten. (15 hp)
488. Henriksson, Oskar, 2016: The Dynamics of Beryllium 10 transport and deposition in lake sediments. (15 hp)
489. Brådenmark, Niklas, 2016: Lower to Middle Ordovician carbonate sedimentology and stratigraphy of the Pakri peninsula, north-western Estonia. (45 hp)
490. Karlsson, Michelle, 2016: Utvärdering av metoderna DCIP och CSIA för identifiering av nedbrytningszoner för klorerade lösningsmedel: En studie av Färgaren 3 i Kristianstad. (45 hp)
491. Elali, Mohammed, 2016: Flygsanddyners inre uppbyggnad – georadarundersökning. (15 hp)
492. Preis-Bergdahl, Daniel, 2016: Evaluation of DC Resistivity and Time-Domain IP Tomography for Bedrock Characterisation at Önneslöv, Southern Sweden. (45 hp)
493. Kristensson, Johan, 2016: Formation evaluation of the Jurassic Stø and Nordmela formations in exploration well 7220/8-1, Barents Sea, Norway. (45 hp)
494. Larsson, Måns, 2016: TEM investigation on Challapampa aquifer, Oruro Bolivia. (45 hp)
495. Nylén, Fredrik, 2017: Utvärdering av borrhålskartering avseende kalksten för industriella ändamål, File Hajdarbrottet, Slite, Gotland. (45 hp)
496. Mårdh, Joakim, 2017: A geophysical survey (TEM; ERT) of the Punata alluvial fan, Bolivia. (45 hp)
497. Skoglund, Wiktor, 2017: Provenansstudie av detriala zirkoner från ett guldförande alluvium vid Ravlunda skjutfält, Skåne. (15 hp)
498. Bergcrantz, Jacob, 2017: Ett fönster till Kattegatts förflutna genom analys av bottenlevande foraminiferer. (15 hp)
499. O'Hare, Paschal, 2017: Multiradionuclide evidence for an extreme solar proton event around 2610 BP. (45 hp)
500. Goodship, Alastair, 2017: Dynamics of a retreating ice sheet: A LiDAR study in Värmland, SW Sweden. (45 hp)

LUNDS UNIVERSITET

Geologiska institutionen
Lunds universitet
Sölvegatan 12, 223 62 Lund